NASA CONTRACTOR
REPORT

NASA CR-61317

SPHERE FORMING AND COMPOSITE CASTING IN ZERO-G

Arthur D. Little, Incorporated
Cambridge, Massachusetts

January 7, 1970

Final Report

Prepared For

NASA-GEORGE C. MARSHALL SPACE FLIGHT CENTER
Marshall Space Flight Center, Alabama 35812

TECHNICAL REPORT STANDARD TITLE PAGE

1. REPORT NO.	2. GOVERNMENT ACCESSION NO.	3. RECIPIENT'S CATALOG NO.
NASA CR-61317		

4. TITLE AND SUBTITLE	5. REPORT DATE
Sphere Forming and Composite Casting in Zero-G	January 7, 1970
	6. PERFORMING ORGANIZATION CODE
7. AUTHOR(S)	8. PERFORMING ORGANIZATION REPORT # 70538
9. PERFORMING ORGANIZATION NAME AND ADDRESS Arthur D. Little, Inc. Cambridge, Mass.	10. WORK UNIT NO.
	11. CONTRACT OR GRANT NO. NAS 8-21402
12. SPONSORING AGENCY NAME AND ADDRESS NASA-George C. Marshall Space Flight Center Marshall Space Flight Center, Alabama 35812 Manufacturing Engineering Laboratory	13. TYPE OF REPORT & PERIOD COVERED Contractor Report
	14. SPONSORING AGENCY CODE

15. SUPPLEMENTARY NOTES Distribution of this report is provided in the interest of information exchange. Responsibility for the contents resides in the author or organization that prepared it.

16. ABSTRACT

SEE THE SUMMARY SECTION

17. KEY WORDS	18. DISTRIBUTION STATEMENT
	STAR Announcement

19. SECURITY CLASSIF. (of this report)	20. SECURITY CLASSIF. (of this page)	21. NO. OF PAGES	22. PRICE
U	U	122	

FOREWORD

The program described in this report was conducted by Arthur D. Little, Inc. (ADL) for the National Aeronautics and Space Administration, George C. Marshall Space Flight Center, under Contract NAS8-21402. The principal ADL staff members who contributed to the program were: Dr. Alfred E. Wechsler, Dr. J. Berkowitz-Mattuck, Dr. L. Griffiths, Mr. P. C. Johnson, and Mr. R. J. Carroll. The authors gratefully acknowledge the assistance and guidance of Mr. W. E. Hasemeyer, Technical Monitor, and Mr. R. Hoppes of the Manufacturing Engineering Laboratory, NASA-MSFC throughout the program. Consultants to Arthur D. Little, Inc., who contributed to the program were Professors C. Smith, M. Fleming, and A. Sarofim of the Massachusetts Institute of Technology and Mr. S. Bradstreet, an independent consultant.

TABLE OF CONTENTS

LIST OF FIGURES

LIST OF FIGURES (cont'd)

LIST OF TABLES

SUMMARY

BACKGROUND

The reduced gravity in orbiting spacecraft and the high vacuum available having indicated the possibility of manufacturing and materials processing in space, the Manufacturing Engineering Laboratory (MEL) of NASA-MSFC proposed several experiments to demonstrate the feasibility, the practicability and the technical and economic justification for such processes. Experiments M492 and M493 were already being developed for joining materials in space by electron beam welding and exothermal tube brazing; a prototype electron beam and vacuum chamber facility had been developed and isothermal heating devices had been prepared. Consequently, the Manufacturing Engineering Laboratory decided to also use this facility and equipment for sphere forming and composite casting experiments, since the formation of spheres in the zero-g environment might enhance their surface finish, sphericity, hardness, and microstructural properties and the casting of composites might provide better fiber alignment and a more homogeneous structure which could yield improved strength. Solidification of spheres in zero-g might result in a finer, less segregated microstructure because of homogeneous nucleation. Directional solidification of monotectic or eutectic composites could result in materials which not only have improved strength, but unique optical, magnetic, electrical or super-conducting properties. Furthermore, these experiments could provide insight into the mechanisms of solidification and composite formation.

The basic concepts of the sphere forming and composite casting experiments were formulated by the Manufacturing Engineering Laboratory. However, the materials and materials combinations, the details of the heating or melting methods, and the parameters to be studied in these experiments had to be carefully identified and selected to insure that the manufacturing technology experiments would be acceptable to the science and engineering community and could be conducted successfully in the planned materials processing facility within the scope of the approved program.

PURPOSE AND SCOPE

The objective of Arthur D. Little's program was to assist the Manufacturing Engineering Laboratory in the design definition of the sphere forming and composite casting experiments for the AAP Orbital Workshop. The program consisted of:

- Preparation of experiment guidelines and performance criteria

- Identification and preliminary screening of candidate materials and methods
- Laboratory experiments
- Analysis of experiment parameters
- Preliminary design of flight hardware

We used initial planning information provided by MEL on the sphere forming and composite casting experiments to formulate hardware development guidelines--weight, volume, power, sample heating and solidification methods, and experiment configuration--and experiment performance criteria--astronaut commitment, safety, and measurement of experiment success.

We screened a large number of candidate materials and methods on the basis of such considerations as experiment simplicity, astronaut safety, heat transfer methods, potential demonstrability of advantages of zero-g processing, and anticipated hardware requirements. Our selection of materials and methods for the sphere forming experiment was confirmed by a laboratory program in which candidate metals were melted by both rf and electron beam sources--melting and solidifying on stings and drop casting--and the resultant spheres examined to determine their sphericity, hardness, and microstructure. We conducted vaporization experiments to determine the stability of the samples during melting. Our selection of materials, methods, and flight hardware parameters for the composite casting experiment was based upon laboratory experiments in which candidate materials were directionally solidified and the resultant samples examined metalographically.

Analyses of heating and cooling rates, methods for detachment of spheres from their supports, and the effects of residual acceleration were used to guide the design of the flight hardware.

Using results of these laboratory measurements and analyses, we prepared engineering drawings to illustrate the hardware concepts for both the sphere forming and composite casting experiments.

RESULTS

Preparatory Studies

Experiment Guidelines -- The sphere forming and composite casting experiments, performed within the chamber of the Materials Melting Facility, will be based on the following guidelines and criteria:

- Electron beam and exothermic heating will be used for sphere forming and composite casting, respectively.

- Test samples will be mounted in modular design frames which permit installation in the chamber by the astronaut.

- Remote positioning of samples in the electron beam and photography will be the principal astronaut manipulative activities in the sphere forming experiment; the composite casting experiment will require only sequential initiation of the exothermal heaters.

- Gas pressure in the facility will range from 10^{-4} to 10^{-6} torr; sample outgassing will be minimized by pretreatment and materials selection.

- The residual gravity field in the chamber will be about 10^{-5}g, astronaut movement and spacecraft rotation to be the principal determinants of this field.

- Duplicate samples of each material will be provided to enhance experiment success.

- If possible, "free float" conditions will be used in sphere forming to maximize the scientific and engineering benefits from the experiments.

Heat Transfer -- One-centimeter-diameter samples of most useful materials can be melted with the electron beam in less than 20 seconds. Solidification of these samples by radiation cooling will take 2 to 400 seconds; samples with low melting points and low thermal conductivities require the longest times. The long solidification times limit the use of free float conditions to those materials with high melting points. By proper choice of the size and composition of the sting material which supports the samples, relatively uniform cooling and solidification can be obtained in samples held captive on the sting. The exothermal heaters presently under development should be capable of providing the heating rates, temperature distributions, and cooling rates required for composite casting experiments.

Sphere Forming Experiment

Materials -- Although it is unlikely that all the goals of the sphere forming experiment can be met with a single material, many materials show promise of demonstrating the benefits of zero-g fabrication. The lack of buoyancy and thermal convection, plus the prominence of surface tension forces, can produce unique materials as a result of improved nucleation and decreased segregation during solidification. The materials that we screened for their potential in the sphere casting experiment were ferrous alloys, cobalt base alloys, refractory oxides and carbides, aluminum-copper and nickel alloys, and pure metals. In labora-

tory tests we examined samples of aluminum-copper, nickel-tin, and cobalt-chromium-molybdenum alloys; and maraging, low alloy, and and stainless steels. We found that the most desirable materials for the flight experiments were Star "J" Stellite, 350T maraging steel, nickel-12% tin alloy, and pure nickel. Several of these could produce spheres of good surface finish, sphericity, and hardness--perhaps on high as Rc = 60. Others will provide very interesting demonstrations of the effects of zero-g on solidification phenomena.

Methods -- We considered several methods for forming spheres: formation on stings with the sphere held captive or detached after melting; formation in viscous metals; formation of solid or hollow spheres in containers; and formation of spheres by melting wires or tubes. Laboratory experiments and analyses showed that with an electron beam source the most desirable technique would be to melt the samples on stings without detachment (captive sting) or to provide for self-detachment of the spheres from the stings. We examined several techniques for detaching molten spheres from stings and concluded that, for the first flight experiment, automatic self-detachment using surface tension as a driving force and non-wetting stings was the most attractive alternative. Solidification times for low-melting materials are expected to be greater than 100 seconds, thereby precluding the self-detachment method for all but metals with high melting points.

Hardware Design -- The flight hardware for the sphere forming experiment includes a baseplate and cover which together form a container for the samples and the positioning mechanism (Fig. 1). The container can be attached either outside for storage or within the Metals Melting Facility during the experiment. Eighteen samples (at least four of each of Star "J" Stellite, 350T maraging steel, nickel-12% tin, and nickel) are arranged on a wheel-like cylindrical holder that is initially packed in foam within the container. After separating the cover, the astronaut removes the sample holder and mates it with an 18-position stepping motor (or gear drive) mounted to the experiment baseplate. The complete assembly is then mounted within the chamber. The astronaut can remotely move each sample into the electron beam in sequence. The samples can be viewed and photographs taken through a port in the chamber. The design permits accurate positioning within the electron beam and maximum space for the free float experiment, and is compatible with applicable weight and volume constraints. At the conclusion of the experiment, the astronaut recovers the baseplate and sample holder and any detached spheres and reassembles them within the covered container.

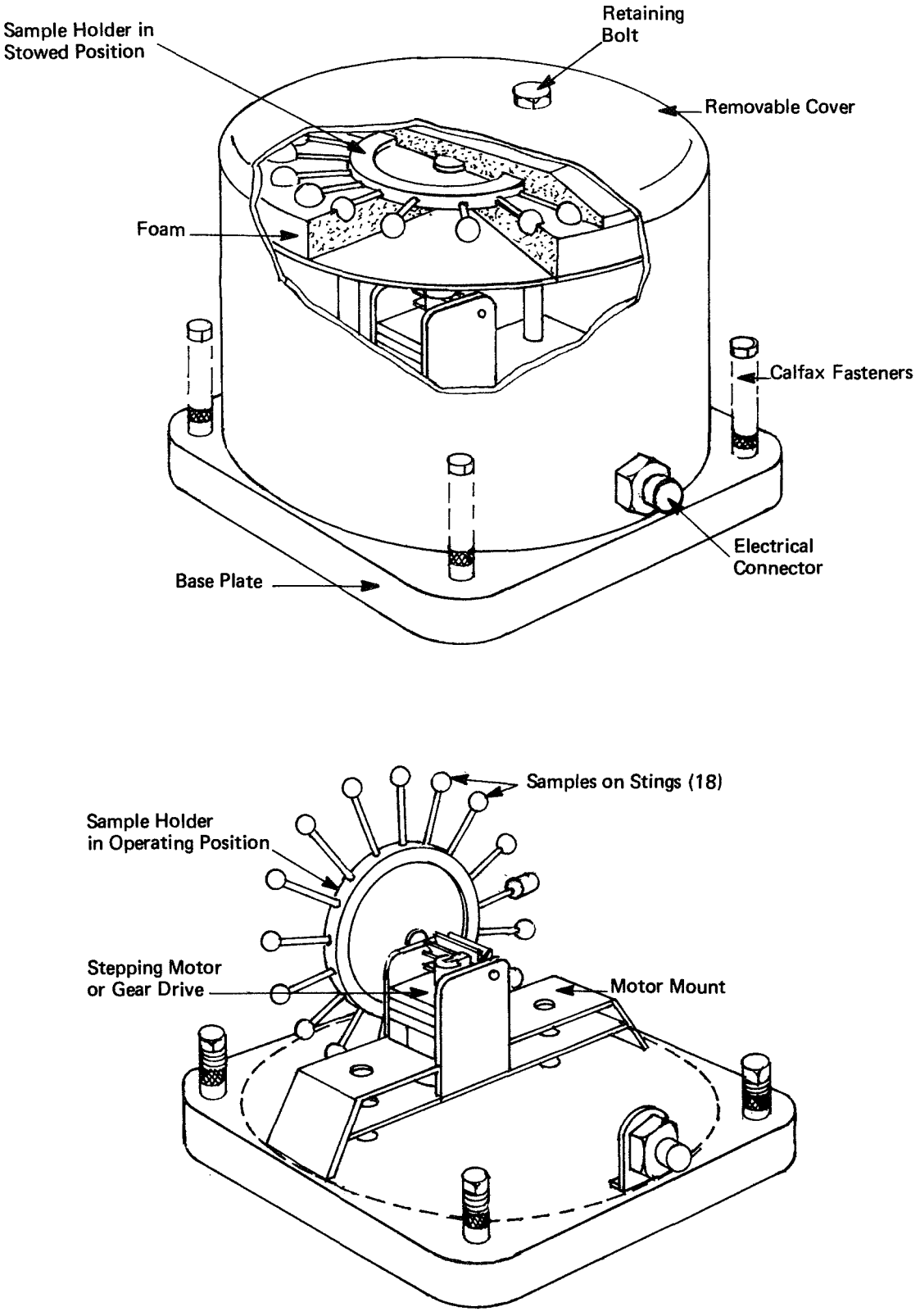

Note: Electron beam perpendicular to plane of sample holder.

FIGURE 1 SPHERE-FORMING EXPERIMENT

Composite Casting

Materials -- The absence of buoyancy and convection in zero-g promised to be of particular benefit to the formation of particle-dispersed, filament-reinforced, monotectic- and eutectic-based composite materials. Therefore, we concentrated our screening on candidate materials such as: TD-Ni and TD-Ni-Cr; SiC whiskers in Al or Mg-35% Al; Al_2O_3 whiskers in Al and $CuAl_2$-Al; C whiskers in Al; Cu-Pb, Al-In, Nb_3Sn-Sn, and Bi-Bi_2Se_3 monotectics; Al_3Ni-Ni, $CuAl_2$-Al, Pb-Sn, InSb-Sb, NiSb, Pb-4% Bi, NaF-LiF, Co-Y_2Co_{17}, and Ni-Ni_3Sn eutectics. We conducted laboratory directional solidification experiments on aluminum-copper, lead-tin, indium-antimony, cobalt-yttrium eutectics; niobium-tin, copper-lead, and aluminum-indium monotectics, and prepared melts of silicon carbide and aluminum oxide whiskers in aluminum or aluminum-copper alloys. Based on these experiments, we selected aluminum-17.3% indium monotectic and aluminum-33% copper eutectic for directional solidification experiments in space. Aluminum-indium has the potential for demonstrating the effects of zero-g on the formation of a rod-like composite. Aluminum-copper will demonstrate the effects of zero-g on the formation of a lamellar eutectic in which the components have different densities. Molybdenum-coated aluminum-oxide whiskers in an aluminum or aluminum-copper matrix will permit us to examine the formation of whisker composites in zero-g.

Methods -- The most promising experimental methods among those that we examined were the remelting of metal matrix fiber composites initially formed on earth, directional solidification of monotectic and eutectic composites, and direct melting of particle-dispersed composites. Properly designed and constructed exothermal heaters could provide the temperature and temperature distribution required for directional solidification of the selected monotectic and eutectic composites and remelting of the whisker composites. The samples used in casting composites should be 4 inches long and 1/4 inch in diameter. The exothermal heaters should provide an initial linear temperature distribution from 650°C at the cool end to 950°C at the warm end (30°C/cm gradient). Cooling should maintain this gradient and not exceed 8°C/minute. One temperature distribution and therefore one exothermal heater design is adequate for the three materials combinations to be melted in the flight experiment.

Hardware Design -- The flight hardware for the composite casting experiment consists of a baseplate and cover which together form both a container and the mounting platform for the exothermal heaters and samples (Fig. 2). Six identical exothermal heaters are supported by the baseplate and framework; the samples are two Al-In, two Al_2Cu-Al, and two Al_2O_3 whiskers in Al_2Cu-Al. Tungsten radiating fins are held by springs against the molten samples to provide directional heat loss. The astronaut removes

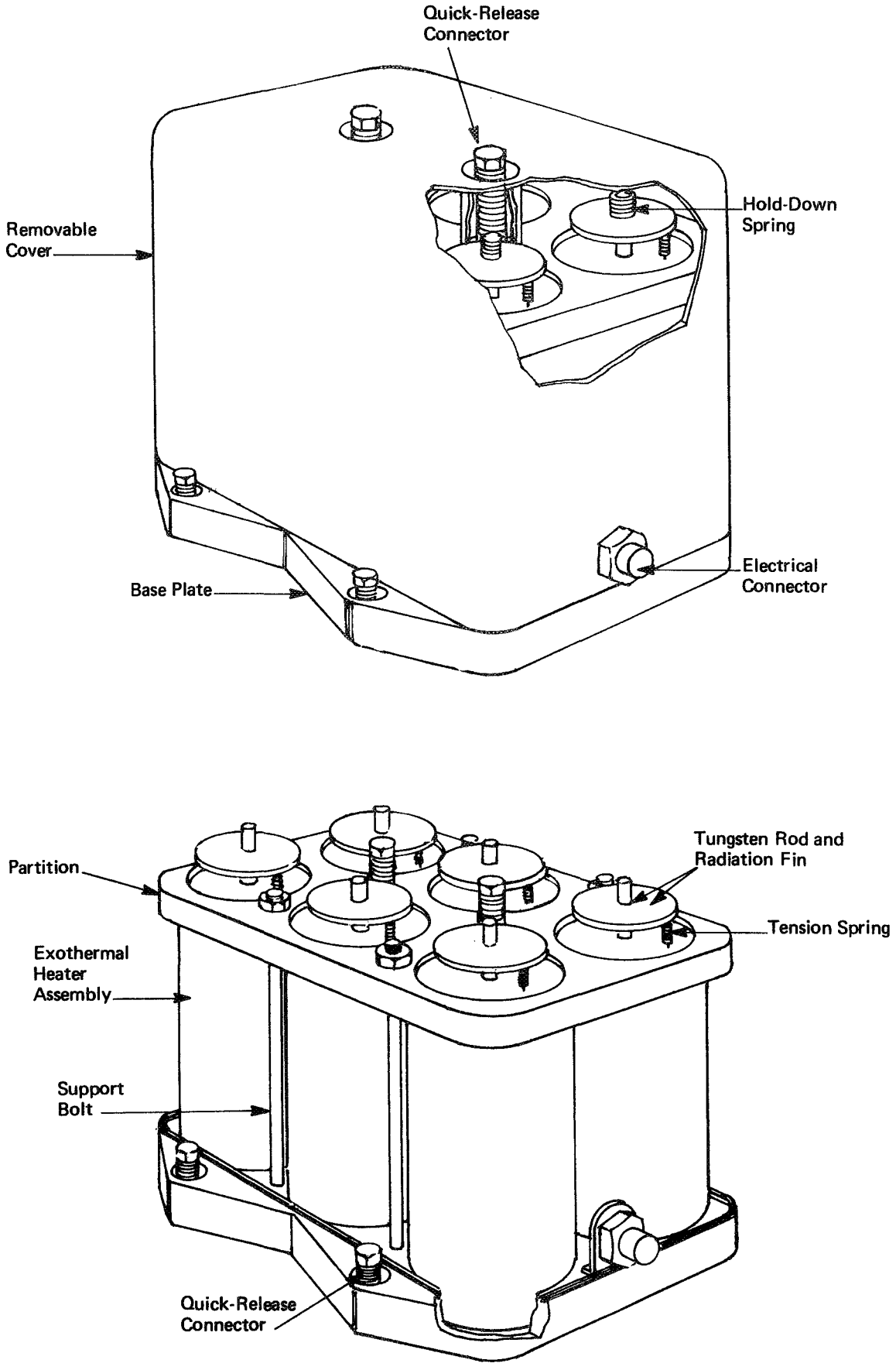

FIGURE 2 COMPOSITE-CASTING EXPERIMENT

the cover and attaches the baseplate within the chamber. The exothermal heaters are turned on remotely; at the conclusion of the experiment the apparatus is removed from the chamber and re-assembled with the cover. The power for the composite casting experiment is self-contained.

PART ONE

PREPARATORY STUDIES

I. EXPERIMENT GUIDELINES

A. HARDWARE CONSIDERATIONS

The composite casting and sphere forming experiments will be performed in the Materials Melting Facility (used in the welding and exothermal brazing experiments). The experiment chamber is a sphere about 16 inches in diameter. The welding and brazing experiments are supported on a cylindrical framework which fits into the chamber. The experiments are arranged so that each of the six or seven materials samples can be remotely rotated in front of the electron beam gun and viewing window. Each of these experiments has a modular design; i.e., an entire new set of samples can be placed in the chamber for each experiment; individual samples can be replaced or interchanged to vary the types of materials studied or to provide duplication of particular materials combinations. Mounting of the framework and position of the specimen are controlled by the astronaut, who will also be responsible for operating the electron beam gun. The astronaut will also control the initiation of the exotherms. Once the experiment has been placed in the chamber, the samples will not be accessible until the experiment framework is removed.

A similar approach was selected for the sphere forming and composite casting experiments. One framework, containing six or more samples, will be used with each experiment. The apparatus must be compatible with the chamber, electron beam gun location, exotherm initiation system, and storage areas. The samples must not interfere with the rotation mechanism or prevent the framework from being removed when the experiment is completed. Materials which are evolved during the experiments should not coat the interior of the viewing window or otherwise restrict photography. A moderate-speed sequence camera will be available to record the sphere forming and composite casting experiments.

Although this program involved only the design of the experiment, NASA's flight fabrication requirements for qualified hardware were carefully considered during the materials selection and design.

B. ENERGY SOURCES

The guidelines established by the Manufacturing Engineering Laboratory specified the use, if possible, of the electron beam power source for the sphere forming experiment and exothermal heating devices for the composite casting experiment.

The electron beam facility can produce up to 2 kw over a target ranging in size from about 3 to 25 millimeters (1/8 to 1 inch) in diameter. The flux is variable from 1 to 2 kw. Experiments to date have shown that defocussing the beam is an effective method

of controlling the energy density. The electron beam source can be operated continuously only for 4-1/2 minutes; however, this should not seriously limit the design of the sphere forming experiment. The sample to be heated must be electrically conductive and grounded, thus limiting the choice of materials which can be used, unless they are contained within a conducting shell heated by the electron beam. Because electrical power must be conserved and because the electron beam source cannot be operated at low power levels, the heating and cooling rates of the samples will be controlled by appropriate design of the sample and shielding rather than by direct heating control. A serious disadvantage of the electron beam heating method is its directionality. Unless a shield or shell surrounds the specimen, heating will take place only over a hemisphere, resulting in temperature gradients in the sample.

The exothermal heaters consist of a mixture of aluminum, boron, and magnesium with vanadium pentoxide, titanium dioxide, nickel oxide, and manganese dioxide. The equivalent heating temperature is over 2000°K. Calculations, based upon the heat of reaction of the constituents, indicate that the energy output of the exotherm is approximately 500 cal/gm. Thus only relatively small quantities of exotherm are required to melt samples up to 1 centimeter in diameter and several centimeters long. Exothermal heating will provide the required uniform flux over the surface of the sample and also slow heating and cooling rates. However, it does sacrifice direct control once the exotherm has been prepared, the access to the sample, and flexibility offered by the electron beam source.

In our evaluation of materials and methods for sphere and composite forming, we have emphasized electron beam and exothermal heaters and considered resistance heating, using the batteries of the electron beam source only in our initial efforts. Calculations of heating and cooling rates, applicable to electron beam and exothermal heaters, are given in Section II.

C. ASTRONAUT CONSIDERATIONS

The essential and extensive contributions of the astronauts in performing experiments in all phases of the Mercury, Gemini, and Apollo programs are well known. Thus, one of the objectives in these materials processing experiments is the effective use of man in space. Sample positioning, heating, photographic control, and experiment coordination and judgment will be the principal astronaut functions in the sphere forming and composite casting experiments. However, because of the many demands placed on astronaut time and function in the workshop program, the experiments should not require complex manipulation, excessive time commitment, or low priority peripheral measurements or control functions.

The safety of the astronaut must be considered in all aspects of the experiment. Materials that are potentially toxic, extremely reactive, or flammable in the oxygen atmosphere of the workshop should be avoided.

Exothermal heaters will obviously be potential astronaut hazards; careful design and qualification testing of these components will be essential. As the experiment progresses, failure modes and hazards will have to be analyzed; however, careful planning and selection of the materials and experiments will prevent the need for modifications at later dates.

D. RESIDUAL GRAVITY FIELD

Although it would be desirable to conduct all materials experiments in the workshop program in as close to zero-gravity as possible--e.g., a free floating condition--it will not be possible, since there will be a residual gravity field in the workshop caused by the radial gradient of the earth's gravity, the rotation of the spacecraft, and the local mass distribution in the spacecraft. The materials in the Materials Melting Facility will also be subject to accelerations, caused principally by astronaut movements and rotation of the workshop. The acceleration of the chamber caused by rotation about the spacecraft axis is expected to be about 10^{-6} to 10^{-5}g. Astronaut movement is also expected to produce accelerations of about 10^{-5}g. Such accelerations would result in translation of a free floating sample relative to the chamber of about two inches in ten seconds. Thus, the sample would soon collide with the chamber or part of the framework, possibly before solidification. During critical experiments that require free floating conditions it will be necessary to restrict astronaut movement.

We postulated that either the sample will be attached to the chamber or framework during both melting or forming or it will be attached during melting but not during solidification. We did not consider levitation and position control of specimen location by rf energy or astronaut manipulation because of the additional electrical power required, the complexity of the system, and the additional astronaut requirements. Position control should certainly be examined in future efforts, but may be eliminated in the initial materials processing experiments.

E. CHAMBER PRESSURE

Present plans indicate that the Materials Melting Facility will be connected to space with a four-inch pipe and valve. At orbital altitudes of 150 and 300 kilometers, the mean atmospheric pressures are about 4×10^{-6} and 1.5×10^{-7} torr, respectively. Because of the conductance of the four-inch line and the natural leakage rate of the spacecraft, the minimum pressure in the chamber may be as high as 10^{-5} torr. Since the electron beam system does not

operate effectively at chamber pressures greater than 10^{-4} torr, the amount of outgassing which can be tolerated in the chamber during heating and forming operations, if the electron beam source is used, is small. Samples must therefore be selected to have low vapor pressures at the melting point and to have limited outgassing products that could fog the viewports or provide electrical conduction leakage paths which interfere with the electron beam operation. Although the chamber pressure is not as critical for exothermal heating, precautions must be taken to avoid vaporization and condensation effects which would restrict subsequent use of the electron beam.

F. MATERIALS CONSIDERATIONS

The objective of the sphere forming experiment is to demonstrate the ability to prepare materials in spherical shapes which cannot be produced on earth to the desired accuracy, uniformity, sphericity, etc. Ideally, the spheres should meet the following requirements: hardness, Rockwell C of 60; roughness, 1 microinch; tolerance, 5 microinch diameter; structure, homogeneous; mechanical properties, similar to ball bearings. In the low gravity of a spacecraft, it is anticipated that solidification under controlled conditions may result in almost perfect spheres and that it might be possible to produce hollow spheres with uniform wall thickness. However, because of the many constraints in the first experiment, it is doubtful that all of the desired properties can be met. Therefore, in selecting materials and methods for forming spheres, we consider that a successful experiment would be one which produced a single confirmed advancement over terrestrial technology: i.e., spheres of lower mass, greater surface hardness, better surface finish, new or more uniform microstructure, or finer grain structure. We have given only limited consideration to the formation of hollow spheres, even though such an experiment could show great advantages over terrestrial fabrication techniques. We have considered a broad range of materials for forming spheres, not only those presently used in ball bearing manufacture. It will be desirable to use different types of specimens to demonstrate several of these benefits of processing in the earth-orbit environment.

The objective of the composite casting experiment is to demonstrate the ability to process in earth-orbit a composite which has more uniform composition, better density control or whisker alignment, or other improvements over similar products prepared on earth. We have broadened our examination of composite materials to consider not only whisker or fiber composites, but also particle dispersions, and composites formed from monotectic and eutectic solidifications, because these materials may also result in unusual and advantageous structural, magnetic, electrical, or strength properties. In selecting materials for the composite casting, in addition to chemical compatibility of the components of the

composite, an important consideration, we used two criteria: (1) for the matrix and filaments (or dispersion), we chose those materials with significantly different densities which are difficult to prepare on earth because of the effects of buoyancy (2) those monotectic or eutectic materials which may exhibit unusual properties when prepared in zero-g because of lack of convection during solidification.

II. HEAT TRANSFER CONSIDERATIONS

Heat transfer plays an important role in the sphere forming and composite casting experiments for several reasons: (1) each experiment requires that samples be heated to their melting points, (2) many solidification processes require that the processing temperatures be controlled, and (3) many processes are adversely affected by thermal convection. We conducted heat transfer analyses initially directed at answering the following questions concerning the heating, melting, and solidification of sample materials ranging in diameter from one millimeter to one centimeter--the most practical limits for the electron beam focus diameter--using the electron beam source or exothermal heaters:

(1) What are the maximum sample temperatures that can be achieved?

(2) What sample temperatures can be achieved if they are enclosed within a shield?

(3) How much energy is required to melt samples and how long does melting take?

(4) What is the time required for solidification?

(5) What is the effect of a sting or support on the heating and cooling processes?

(6) What are typical temperature gradients in samples during heating?

Subsequently, we analyzed more specific heat transfer problems using sample materials and dimensions selected from the screening procedures and laboratory measurements. (See Parts II and III.)

To answer these questions we examined the melting of several materials with a broad range of thermal properties (Table 1). The selection of these materials for heat transfer calculations did not necessarily mean that they would be used in the sphere forming or composite casting experiments.

A. MAXIMUM SAMPLE TEMPERATURES

The electron beam can be focussed to any diameter from about one millimeter to almost two centimeters. The maximum sample temperature that can be achieved by direct heating with the electron beam can be calculated by equating the available electron beam power to the thermal energy radiated from the sample--i.e., assuming negligible conduction heat loss (gas conduction and convection will be eliminated because of the vacuum). Thus:

TABLE 1

THERMAL PROPERTIES OF TYPICAL MATERIALS

Material	Thermal Conductivity (watt/cm °K)	Density (gm/cm^3)	Specific Heat (cal/gm°C)	Thermal Diffusivity (cm^2/sec)	Heat of Fusion (cal/gm)	Melting Point (°K)	Emittance
Tungsten	1.1-1.5	19.3	0.040	0.33	46	3643	0.3
Copper	3.5	8.9	0.087	1.1	51	1356	0.1
Carbon Steel	0.5	7.9	0.11	0.15	64	1790	0.2
Aluminum Oxide	0.35-0.06	4.0	0.2-0.3	0.02-0.09	260	2050	0.1
Titanium Carbide	0.21-0.04	4.9	0.22	0.01-0.06	334	3410	0.8
Aluminum	2.2	2.7	0.22	0.87	95	933	0.1

$$q_{eb} = \pi d^2 \varepsilon \sigma T_s^4 \qquad (1)$$

where: q_{eb} = electron beam power

d = specimen diameter

ε = emittance

σ = Stefan-Boltzman constant

T_s = sample temperature

For samples two millimeters and one centimeter diameter, respectively, using an average electron beam power of one kilowatt, we calculated the maximum temperatures (Table 2).

TABLE 2

CALCULATED MAXIMUM TEMPERATURES WITH ELECTRON BEAM HEATING (°K)

Diameter/Emittance	0.1	0.2	0.3	0.8	1.0
2 mm	>6500	>6500	>6500	6500	6200
1 cm	4900	4100	3700	2900	2750

Looking at Tables 1 and 2 we see that almost all 1-cm-diameter samples could be melted with an output of 1 kw in the electron beam if their melting points were below 2750°K. However, a 1-cm-diameter tungsten sample might not be melted because of its high melting point; a 1-cm-diameter titanium carbide sample could not be melted because of its high emittance. If any of the samples are enclosed in a 1-cm-diameter graphite shield, a temperature of 2750°K could be attained. If the graphite shield were 2 cm in diameter, a temperature of 1950°K could be reached at 1 kw power, or 2300°K at 2 kw power. These calculations, particularly the high temperatures indicated for small samples, emphasize the conclusions that (1) most materials in samples up to 1 cm in diameter can easily be melted by the electron beam and (2) careful control of the electron beam will be required to prevent vaporization of small samples.

The exothermal heaters will surround the composite casting samples almost completely; therefore, the maximum sample temperature will be limited only by the exothermal reaction temperature and the quantity of exothermic material present. We estimate this maximum temperature to be about 2000°K.

B. MELTING OF SAMPLES

The electron beam (Table 3) can produce about 2000 joules per second continuously for a maximum of about 4-1/2 minutes, therefore, as indicated in Table 3, the energy required to melt samples is well within the capability of the equipment.

TABLE 3

CALCULATED ENERGY REQUIRED TO MELT SPHERICAL SAMPLES (JOULES)

	2-cm diameter	1-cm diameter	2-mm diameter
Tungsten	15,500	1,940	15
Copper	8,000	1,000	8
Carbon Steel	8,900	1,110	9
Aluminum Oxide	18,200	2,300	18
Aluminum	4,500	560	45

If the samples were perfectly shielded (i.e., no heat loss), one or two seconds would be sufficient to melt 1-cm-diameter samples with the electron beam. However, unshielded samples can radiate to the surroundings, thereby increasing the heating and melting time.

We estimated the heating and melting times for unshielded samples by the following procedure. We assumed that the spherical samples were isothermal (high thermal conductivity) and radiated to a cold surrounding (T_o), and that the applied power from the electron beam (q_{eb}) was constant. Then by equating the heat input to the radiative losses and the change in temperature of the sphere:

$$q_{eb} = MC \frac{dT_s}{d\theta} + A\,(\varepsilon\sigma T_s^{\,4} - \alpha\sigma T_o^{\,4}) \qquad (2)$$

where: M = mass of sphere = $\frac{\pi d^3 \rho}{6}$

C = specific heat

A = surface area of sphere = πd^2

α = absorptivity of surroundings = 1

$dT_s/d\theta$ = rate of change of temperature of the sphere

Assuming that density and thermal properties are constant with temperature, and letting $T_2 = T_o^4 + q_{eb}/A\varepsilon\sigma$, Equation 2 was rearranged and approximated as:

$$\frac{dT_s}{d\theta} \approx \frac{6\varepsilon\sigma}{d\rho C} (T_2^4 - T_s^4) \tag{3}$$

and

$$\int_{T_{s,i}}^{T_M} \frac{dT_s}{T_2^4 - T_s^4} \approx \frac{6\varepsilon\sigma}{d\rho C} \theta_M \tag{4}$$

where: $T_{s,i}$ = sphere initial temperature

T_M = melting point

θ_M = time required to reach melting point

Equation 4 can be integrated easily to determine θ_M. (Note that Equation 4 is valid only if $T_o^4 << q_{eb}/\pi d^2\varepsilon\sigma$; if the spheres radiate to room temperature and the electron beam power is 1 kw, this is valid for all practical diameters). Table 4 shows the results (the figures without the parentheses) for 1-cm-diameter spheres with a power input of 1 kw totally absorbed by the sample and a surrounding temperature of 300°K. The time for melting, much longer than expected from the heat of fusion alone, was calculated assuming that the electron beam energy available to melt the sample equals the energy absorbed less energy radiated by the sphere at the melting point. In these calculations we assumed that the samples will be at uniform temperature, although they are heated only from one side by the electron beam. This assumption is not justified for material of low conductivity. Therefore, we estimated a warm-up time based on transient thermal conduction from the equation:

$$\theta_M = \frac{d^2\rho C}{k} \tag{5}$$

where: k = thermal conductivity of specimen

Table 4 shows the values for the heating time given by this equation (and the total melting time) in parentheses.

TABLE 4

CALCULATED HEATING AND MELTING TIMES FOR TYPICAL MATERIALS (seconds)

Material	Time For Heating	Time For Melting	Time Total
Tungsten	8.5 (3)	43	52 (46)
Copper	1.7 (1)	1	3 (2)
Steel	2.8 (6)	1.1	4 (7)
Aluminum Oxide	2.3 (62)	2.3	5 (64)
Aluminum	0.83 (1.5)	0.6	1.5 (2.1)

Thus Table 4 shows that transient conduction will be the controlling rate of heat transfer for low conductivity materials such as steel and aluminum oxide. It will be time consuming to melt oxide samples. These calculations also showed that significant temperature gradients could exist across unshielded low-conductivity samples which receive heat from only one side. Most metals we have considered, however, can be melted in less than 15 or 20 seconds. Thermal shielding could be used to shorten melting time and reduce temperature gradients but would prolong cooldown times.

We did not perform explicit calculations to determine exothermal heating times; however, we concluded that the time to melt samples will be about the same as with electron beam heating. The heat input rate will be lower and the exothermal furnaces will have considerable thermal inertia, but the samples will be heated over the entire surface.

C. SOLIDIFICATION OF SAMPLES

Although the heating and melting rates of the samples are relatively rapid because of the high heat flux available, the rates of cooling and solidification are governed by the optical properties of the molten material, the conductive and radiative losses, and the heat capacity of the exothermic heaters. To estimate the maximum solidification times, we assumed that the spherical samples were coupled with the environment by radiation only. The solidification time was calculated by equating the radiative losses and the heat of fusion:

$$\theta_s = \frac{\rho \Delta H d}{6 \varepsilon \sigma T_M^4} \qquad (6)$$

where: θ_s = solidification time

ΔH = heat of fusion

T_M = melting point

Table 5 shows the calculated solidification times for 1-cm-diameter spheres.

TABLE 5

CALCULATED TIME REQUIRED TO SOLIDIFY 1-CM-DIAMETER SPHERES

Material	Solidification Time (sec)
Tungsten	2.2
Copper	165
Steel	30
Aluminum Oxide	70
Aluminum	400

Long times are required because of the relatively low melting points of copper and aluminum, and the corresponding low radiation heat transfer rates. Note that the solidification time is directly proportional to the diameter. Shielding samples would further increase the cooling time; a single shield with an emittance of 0.1 would more than double the cooling time. The long cooling time for the low-melting-point materials seriously limits their use in free float conditions, and indicates that low-melting-point samples will have to be held on stings or supports.

If the sphere forming samples are held on a sting, the uniformity of cooling will be determined by choice of the sting size and material. To evaluate the uniformity of cooling of samples, we estimated the ratio of heat loss by conduction along the sting to heat loss by radiation over the surface of the sample. For simplicity, we considered an unshielded spherical sample at its melting point and determined the maximum ratio of conductive losses (Q_{cond}) to radiative losses (Q_{rad}) as follows:

$$Q_{rad} = \pi d^2 \sigma \varepsilon \, (T_M^4 - T_o^4) \qquad (7)$$

where T_o = radiation sink temperature = 300°K.

$$Q_{cond} = \frac{\pi k_s d_s^2}{4} (T_M - T_o) \sqrt{\frac{4h}{d_s k_s}} \qquad (8)$$

where: k_s = thermal conductivity of the sting

d_s = diameter of sting

h = heat transfer coefficient from sting surface

In this analysis, the sting acts like a fin. We assumed that the sting is long and is connected to a heat sink at T_o. If the sting radiates to the sink at T_o, the maximum heat transfer coefficient is given approximately as:

$$h = \frac{\varepsilon_s \sigma T_M^4}{T_M - T_o} \qquad (9)$$

where: ε_s = emittance of sting

In these estimates we assumed that gas conduction and convection were negligible. Table 6 shows typical results for several materials combinations and sample sizes. As the sting diameter decreases, the conduction losses decrease. For the same ratio of sphere to sting diameter, the smaller the sphere the greater the ratio of conduction to radiation losses, suggesting that for most materials uniform cooling will be possible with small stings. For copper and aluminum specimens, a low-conductivity sting will be required to have uniform cooling; because of the low thermal conductivity of steel alloys, larger stings can be used to achieve the same uniformity than with copper or aluminum alloys. Sphere diameters of 0.5 cm with stings of 0.01 cm (0.004") seem practical. It may also be necessary to have the samples carefully packaged during launch operations, and have them attached or assembled by the astronaut.

TABLE 6

RATIO OF CONDUCTION TO RADIATION HEAT LOSS DURING SAMPLE SOLIDIFICATION FOR VARIOUS DIAMETER SPHERES AND STINGS

Material Combination	Sphere and Sting Diameters: Sphere = 1 cm, Sting = 0.1 cm	Sphere = 1 cm, Sting = 0.01 cm	Sphere = 0.5 cm, Sting = 0.01 cm	Sphere = 0.1 cm, Sting = 0.01 cm
Sphere and Sting of Same Material				
Tungsten	0.055	0.002	0.007	0.17
Copper	0.69	0.022	0.087	2.2
Steel	0.04	0.001	0.005	0.13
Aluminum Oxide	0.03	0.001	0.004	0.10
Aluminum	0.87	0.028	0.11	2.8
Sphere and Sting Different Materials				
Sphere - Copper Sting - Tungsten	0.67	0.021	0.082	2.1
Sphere - Copper Sting - Alumina	0.29	0.009	0.036	0.90
Sphere - Aluminum Sting - Tungsten	1.0	0.034	0.14	3.4
Sphere - Aluminum Sting - Alumina	0.46	0.015	0.060	1.5
Sphere - Steel Sting - Tungsten	0.23	0.007	0.029	0.73
Sphere - Steel Sting - Alumina	0.097	0.003	0.012	0.31

PART TWO

THE SPHERE FORMING EXPERIMENT

III. BACKGROUND

The principal earth-orbit environment factors that are expected to alter the present technology of solidification are low or zero-g and high vacuum--zero-g being by far the most significant. Vacuum melting and casting have become accepted practice on earth where the superior quality of the end product can be economically justified. The zero-g environment, however, can only be approximated on earth in the laboratory by such techniques as electrostatic suspension and inductive levitation, and then only on small samples and with great difficulty.

The zero-g environment is expected to have several effects on solidification. Of primary interest to our objectives for the sphere forming experiment is the increased prominence of surface tension forces in the zero-g environment so that, in principle, it should be possible to carry out containerless solidification of a perfectly spherical shape.

A principal goal of the materials processing experiments is, therefore, to cast a sphere having the following characteristics:

- Metallurgy--a homogeneous structure, a minimum hardness of Rc 60, and mechanical properties comparable to those of ferrous ball bearings.
- Surface roughness--not to exceed 1 microinch.
- Diameter variation--not to exceed 5 microinches.
- Low mass--preferably a hollow sphere of uniform wall thickness.

Sample materials and experimental techniques for forming spheres must be evaluated not only in terms of their ability to fulfill this goal, but also in the light of their applicability to scaled-up manufacturing. Furthermore, the zero-g environment will have profound effects on solidification phenomena, other than the formation of spherical shapes. Where possible, the sphere forming experiment should be designed to determine if unique and useful structures can be prepared.

It is unlikely that all the desired product characteristics can be met by a single material or a single forming technique in the initial flight experiments. It may, however, be possible to meet many of the requirements with experiments that are also designed to critically evaluate experimental procedure and solidification phenomena.

A. METALLURGY

This goal cannot be met entirely. The mechanical properties of ferrous ball bearings and the homogeneity of the structure are the result of mechanical work and subsequent heat treatment of the cast material. The as-cast structure of alloyed steels is nonhomogeneous because of redistribution of the alloying elements on freezing. However, it may be possible to produce load-bearing rolling elements which are useful in the as-cast condition even though they may not meet all the desired properties.

B. SURFACE ROUGHNESS

Because of the volume change associated with solidification, some surface roughness will invariably result in bearing alloys if the outer surfaces are free cast. This problem might be avoided using an experimental technique which removes the surface roughness after the metallic surface has solidified. Alternatively, this goal may be approached by the use of a model system, either a very pure metal or an alloy whose volume change is nearly zero.

C. SPHERICITY

Attainment of sphericity is primarily an experimental problem. Lack of sphericity could be caused by nonuniform heating, nonuniform cooling, nonuniform solidification leading to internal stresses, or oscillation in the melt due to deviation from zero-g or forces induced by specific experimental techniques. Again, model materials could be chosen having appropriate properties (viscosity, surface tension) such that a ball diameter could be chosen which would meet the goals.

D. LOW MASS

Casting of a hollow ball is also primarily an experimental problem. Although there are techniques which might lead to such a product, there is no reason to believe that the cavity will center itself in the ball. Furthermore, the sphericity will be affected to the same extent by the factors described above. An alternate approach would be to cast around a low-density, low-modulus core. Because of the complexities and doubtful outcome of experiments to produce spheres with low mass, we have concentrated our efforts on producing solid spheres in the initial Orbital Workshop experiments.

IV. THE IMPLICATIONS OF SOLIDIFICATION IN A ZERO-G ENVIRONMENT

It is not possible to predict from terrestrial experience whether the difference between a true zero-g environment and the small but finite forces which will exist in the Materials Melting Facility are critical to solidification phenomena. We can, however, define the factors which are likely to be significant to solidification phenomena in zero-g and postulate the characteristics--possibly unique--of the resultant casting. The zero-g environment is expected to affect solidification because buoyancy and the resultant density differences or thermal convection will be non-existent, and therefore surface tension forces will assume a more prominent role.

A. SUPERCOOLING AND NUCLEATION

By solidification of "containerless" melts, a high degree of supercooling may be possible because of the absence of container walls that act as nucleation sites. A variety of pure metals and commercial alloys have been undercooled on earth by amounts up to 200-300°C below their melting points with substantial structural modification and reduction of segregation ratio.[1] Also, a much greater degree of homogenization is possible by subsequent heat treatment of alloys which have been significantly supercooled.[2-6] Since large amounts of undercooling are theoretically possible before the onset of homogeneous nucleation, solidification in the zero-g environment may permit even finer, less segregated structures than are possible on earth. It may even be possible to reach the homogeneous nucleation temperature in melts of a size sufficient to have practical application.

Even if solidification takes place in a container, nucleation phenomena are likely to be quite different in a zero-g environment. Except for the rather specific single-crystal growth techniques, most castings involve more than one nucleus and can exhibit a variety of growth modes. For example, a casting may exhibit a chill zone consisting of very fine equiaxed crystals near the mold walls followed by a columnar zone with another equiaxed zone in the last metal to freeze. Turbulence and convection have been shown to be a major cause of the two equiaxed zones.[7-11]

It is not unreasonable to expect that the effects of zero-g on nucleation phenomena may lead to very unusual cast structures and might even result in a monodendrite monocrystal.

B. SEGREGATION

Segregation effects can be highly influenced by nucleation and growth phenomena. In a zero-g environment segregation will also be significantly modified by the absence of buoyancy and thermal convection. As alloys solidify, there is a redistribution of the alloying elements as the solid-liquid interface advances. The solidification structure depends to a great extent on the composition of the liquid, and this in turn is greatly affected by thermal convection, which causes mixing. In casting metal ingots, equiaxed crystals are sometimes observed in the lower part of the casting with a columnar region at the top. The effect has been ascribed to gravitational settling of the equiaxed grains, or to a sinking of solute-enriched liquid that reduces the constitutional supercooling at the upper part of the interface between the columnar zone and the melt.[12] Segregation due to constitutional density differences should be impossible in zero-g. These same considerations also apply to the microsegregation that occurs with dendritic growth.

The absence of convection should also have a great effect on the size and distribution of inclusions in alloys. The larger inclusions are thought to result from agglomeration of smaller inclusions that contact each other in the melt and become trapped in the dendrite structure.[13] Because coarse inclusions are generally detrimental to the properties of alloys, solidification in zero-g could result in structures having improved properties.

Thus, solidification in a zero-g environment may result in an extremely fine dendrite structure. The segregation ratio may be very low and inclusions may be very fine and uniformly dispersed.

V. PRELIMINARY SCREENING OF MATERIALS AND METHODS

A. CANDIDATE MATERIALS

We considered two criteria for selecting materials as potential candidates for the sphere casting experiments: (1) those which may be capable of meeting all of our specified goals and (2) those which may show particular promise for meeting individual goals for evaluation of experimental techniques, or for providing evidence of the unique aspects of solidification in space.

1. Materials for Hard, Wear-Resistant Spheres

Most hard, high-strength ferrous alloys depend on carbon, either in solution or in the form of carbides, to provide the required mechanical properties. The as-cast structure exhibits a eutectic, which is rich in the brittle carbide phase, particularly in the more highly alloyed steels. The carbide phase and the eutectic are both continuous so that the as-cast ingots are brittle. These steels may be hard in the conventional sense of the word, but they lack touchness. It is for this reason that the hard, high-strength steels for applications requiring some toughness are usually supplied in the wrought condition. The hot work serves to break up the carbide network and homogenize the structure of the steel.[14]

Some homogenization of the as-cast structure is possible by post-heat treatment to dissolve the carbides in the austenite. The finer the scale of the cast structure, the more effective will be such treatment.[2-6] If a large amount of undercooling can be achieved in the zero-g environment, resulting in a fine structure, a given steel composition could possibly be treated to higher toughness levels than it could in a conventional terrestrial casting which has been more slowly solidified.

Nevertheless, the higher carbon steels can probably not be expected to have sufficient toughness in the as-cast condition. In selecting candidate materials from the ferrous alloys we have therefore concentrated on those compositions which may conceivably have the required hardness, yet have as low a carbon content as possible. Most of the candidate compositions are not supplied in the form of castings, so that property data on them are meager. There is, of course, virtually no information available on the engineering properties of castings made at very large amounts of supercooling. The criteria for material selection in this category are thus less explicit and more conjectural. The selection must be based on what types of alloys might be expected to possess the best combination of structure and properties under the various solidification conditions which have been postulated for the zero-g environment. The general criteria are:

- The steel should be low in alloying elements which tend to produce brittle network structures in the as-cast material,

- The materials properties in the cast condition should preferably be useful enough so that the materials are commercially available in that form,

- The need for any subsequent treatment at temperatures where the steel might distort should be avoided, and

- The material be compatible with the experimental apparatus and techniques.

We eliminated one obvious possibility, subsequent carburizing of a tough low carbon steel, because such treatment could probably not be accomplished without some loss of sphericity.

a. Ferrous Alloys

The most extensively used steel grade for bearings is 52100. It combines good strength, hardness, fatigue, and hardenability properties, yet has a low alloying content, and is therefore inexpensive.(15) It has a quite high carbon content, however, and is not likely to have sufficient toughness in the as-cast condition. Two other steels, D6AC and 300M, have a somewhat higher alloying content, and are capable of achieving hardness better than Rc 60 despite a relatively lower carbon content (approximately 0.45%). They are both low alloy steels, so that undesirable solidification structures may be minimized. One advantage of D6AC is that it is classed as an air-hardening steel. Experimental casts of 300M have been successful, although at a lower carbon content,(15) which would decrease the hardness attainable. Both alloys are likely to have lower hardness limits in the cast condition; nevertheless, they are more likely to possess a better combination of hardness and toughness properties than 52100. Astralloy is another low alloy steel of considerable hardness, even in the cast condition.

The 18 Ni maraging grades of steel depend for their strength on a precipitation reaction of titanium and aluminum rather than on carbon. One maraging grade that has a tensile strength of 250,000 psi in wrought form is also available in a casting grade which provides a hardness of Rc 50. This material has very good ductility and toughness. It is possible that the 350,000-psi grade could attain a hardness over Rc 55 yet preserve sufficient ductility to be useful.(16)

Another alloy which is used extensively in its wrought form for bearing components is 440C stainless steel, capable of Rc 60 in its wrought form. Despite its high carbon content, it is used in some investment castings, and may therefore be capable of

yielding a cast sphere having a suitable combination of properties.[15]

The age-hardening stainless steels, of which 17-4 PH and AM-355 are but two examples, also depend on a precipitation reaction to achieve their properties. Many of these alloys are used for investment casting, but they cannot achieve much more than Rc 50 in hardness;[15] therefore, we have eliminated these alloys from further consideration.

Tool steels represent another class of alloys which have been developed for high-strength, high-hardness applications.[17] There is a wide range of these alloys, from low-alloy types similar to the low-alloy high-strength steels to the highly alloyed high-speed and hot-work tool steels. Several of the high-speed compositions are now used for bearing components for high-temperature service. All the tool steels are universally employed in wrought form because of the poor properties of their as-cast structures, which also make some of the more highly alloyed types even difficult to hot roll. Rather than the tool steels, other ferrous alloys--maraging steel, 440C martensitic stainless steel, and low-alloy steel "Astralloy"--have more promise to meet the program objectives.

b. Cast Cobalt-Base Alloys

Cobalt alloys have long been used in applications requiring hardness and wear resistance. Many of them are used in the form of castings. Star J Stellite is a cobalt-chromium-tungsten alloy which has an as-cast hardness of Rc 55-62. Although it is sensitive to stress concentrations, it has shown promise for bearing components at elevated temperatures.[18] This alloy seemed to be one of the more promising for fulfilling the objectives of this program, and warranted further evaluation.

c. Refractory Hard Materials

A number of oxides, carbides, nitrides, borides and intermetallics have shown promise as load-bearing, wear-resistant components.[19,20] Because of the expected experimental difficulties in casting these materials, primarily associated with melting by the electron beam and thermal shock, we eliminated these materials from consideration for the initial materials processing experiments.

2. Materials for Sphericity and Surface Finish

None of the materials which have been discussed thus far is ideal from the standpoint of producing a highly spherical, smooth sphere, basically because the alloys are complex and have only moderate thermal conductivity. A better material would be one of very

high purity, oxide-free or capable of dissolving its oxides when molten, having good thermal conductivity, and having a proven capability for achieving large undercooling. Materials which might be expected to fulfill these requirements are the noble metals, nickel, cobalt, and iron. Of these, nickel appears to be the most attractive in that it has been undercooled as much as 285°C in the laboratory.[21] Not only is a very smooth round sphere possible, but solidification of a pure metal at undercoolings not possible on earth may be achieved.

3. Materials for Evaluating the Effects of Zero-G on Solidification Phenomena

Although all of the materials that have been discussed thus far can be expected to provide evidence of the unique effects of zero-g on solidification phenomena, most of them are complex alloys in which these effects may be difficult to detect. None of them can be expected to accentuate the postulated effects of solidification in zero-g.

A very useful alloy from this standpoint is an aluminum casting alloy, No. 195, which has the composition Al-4.5% Cu. This alloy has a wide freezing range and a large density difference between the two components. It has been studied extensively, and forms the basis of much of our understanding of alloy solidification in gravity. Much information on the structure that results from a wide variety of solidification conditions is available. It is an ideal alloy for investigating those aspects of solidification which may be unique to a zero-g environment.

However, because of its low melting point and long solidification time, it may not be compatible with the experimental techniques. In that event, either Ni-14% Al, Ni-7.5% Al, or Ni-12% Sn could be substituted.

B. CASTING METHODS

In our preliminary screening, we considered four methods of casting spheres: on a sting (or support); within a viscous melt; in a solid container; and by melting of wires or tubes. With one exception we assumed that the electron beam heating would be used and that no mechanical manipulation of the specimen would be possible during the experiment.

1. The Sting Experiment

Considerable preliminary experimental work has already been performed by the Manufacturing Engineering Laboratory using this approach.

a. Captive Sphere

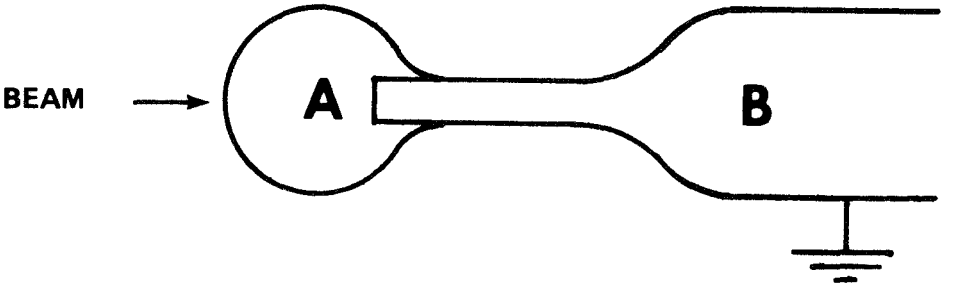

In this technique, the metal sample to be melted is held on the end of the support sting. The objective is to melt the sample without detaching it from the sting, thereby assuring continuous control. The sting must conduct electricity, have a higher melting point than the sphere (material A) and must be wet by material A when molten so that the sphere will not detach.

This technique assures positive control of the sphere, yet provides containerless conditions over the majority of the surface. This technique could be used to obtain a Rc 60 casting, and to optimize the surface smoothness of as-cast metal. However, a perfect sphere cannot be cast by this technique, since the wetting angle must necessarily be less than 90°, and cooling cannot be uniformly radial because of the sting. There will be some alloying of the two materials. The sting will act as a nucleation site, so that the possible advantages of large supercooling will not be attained.

b. Prenecked Sting

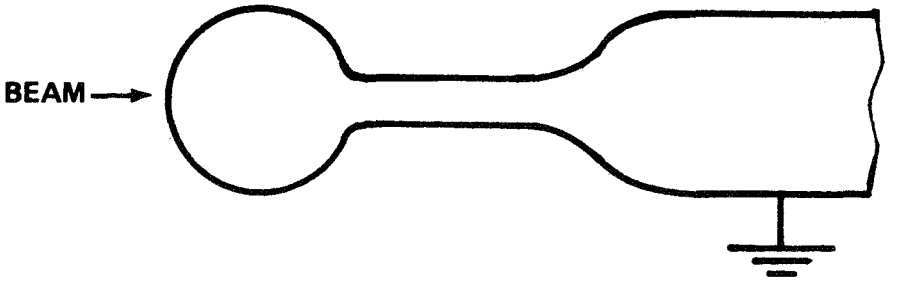

A prenecked sting of a single material is another alternate. As the melt interface proceeds back into the neck, separation of the sphere may occur as a result of thinning of the neck by surface tension forces. The sample material must be an electrical conductor.

This technique avoids many of the problems associated with the captive sphere technique and can be used to meet most of the experiment goals. Materials compatibility problems are avoided. Completion of the experiment is indicated by interruption of the beam current. However, it may be difficult to ensure separation of the sphere in a way which permits it to assume a perfectly spherical shape. There will be temperature gradients on heating and cooling because of beam directionality. It is not certain that the sphere will detach from the sting. If it does, motion may be imparted to the sphere during the separation process, causing it to impact portions of the apparatus before the ball has solidified or becomes hard. Materials will thus be restricted to those which solidify very quickly.

c. Nonwetting Dissimilar Materials

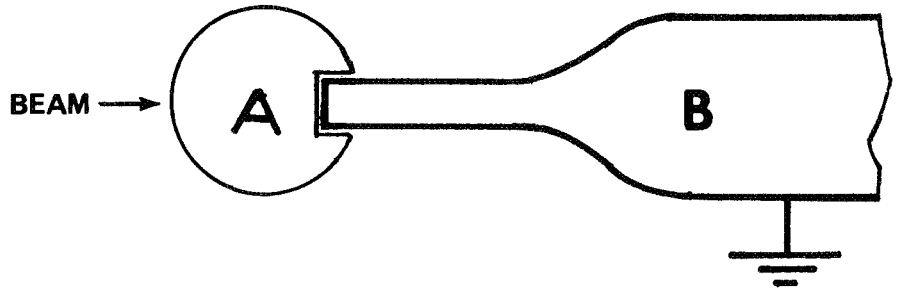

An alternative means of detachment is to use a sphere material, which does not wet the sting. On melting, the sphere will detach itself from the sting to become free floating. Both materials must be electrical conductors, A must not wet B, and B must have a higher melting point than A.

This approach is similar to the prenecked sting experiment; however, separation of the sphere can be better controlled and the temperature gradient problem can be minimized by proper choice of the two materials. The problems with this technique are possible impact of the ball against some portion of the apparatus before it has solidified, and materials compatibility.

d. Other Sting Experiments

We briefly considered the use of a radiation shield surrounding a sample held on a sting as a means for minimizing thermal gradients. This method did not seem appropriate because, if the sphere became detached, it would certainly impact the shield. The technique of casting spheres on low-density solid cores, held captive on stings, offered more disadvantages because of materials compatibility than benefits derived from the overall low density.

2. Spheres Formed in a Viscous Melt

To reduce the possibility of the molten (or soft) sphere from contacting with the walls of a container or the experimental apparatus, a liquid of high viscosity could be used to separate the sphere from its container. The time required for the sphere to contact the container wall would be significantly increased, and the sphere might become sufficiently rigid so that it would not deform on contact. Reaction between the liquid and the sphere could occur and affect the surface smoothness but not necessarily sphericity of the sphere. An encapsulant liquid which offers promise (i.e., the ability to be used over a wide temperature range and still maintain viscosity) is a boron oxide-barium oxide mixture. By varying the composition, a wide range of temperature-viscosity dependence may be obtained. This approach then offers the possibility of using any metal or alloy, regardless of its thermal expansion coefficient, which melts between 800 and 1800°C. The oxide mixture would have to be degassed prior to heating in space; heating the mixture in vacuum to a temperature in excess of the melting temperature of the sphere should suffice.

This approach has the advantage that it reduces the possibility of contact of the hot sphere with components of the apparatus. Temperature gradients are minimized. Through the use of the proper glass, a superior surface finish may result. Although this would not result in containerless solidification, the viscous liquid could be amorphous and may not act as a nucleating site. Therefore, considerable undercooling may still be possible. More than one sphere could be melted per experiment, either of different sizes, or within certain limits, of different alloys. The most significant problem with this experiment is the additional material (viscous melt) which must be heated, and the apparatus size will therefore be limited by the available power. Furthermore this method may not be necessary if spheres could be detached from stings with modest controlled velocities.

3. Melting in a Solid Container

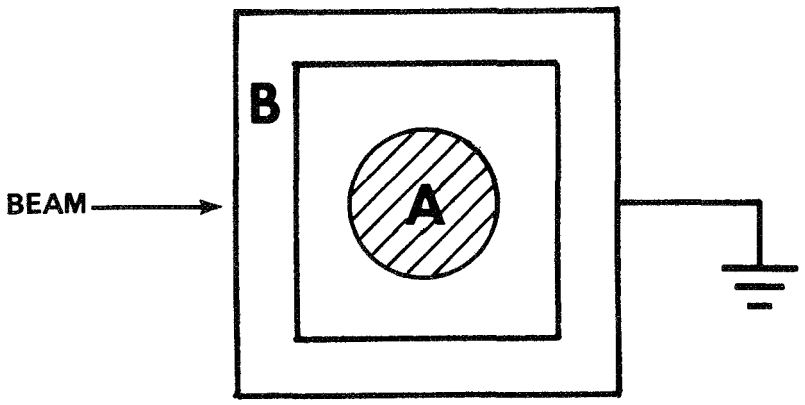

In this method a partially filled container could yield a solid sphere if the sample material when heated and molten is completely nonwetting on the container. This approach could be used to minimize temperature gradients. However, it is doubtful whether a useful metal combination can be found which is completely nonwetting. There is no reason for the sphere to separate from its container for a period sufficient to allow solidification. The power requirements would be high because of the need to heat the container.

An alternative is to melt a metal which partially fills, wets and has a lower melting point than its container. This technique could be used for casting hollow balls. However, the choice of materials is restricted because of materials incompatibility. There is no definite proof that the cavity will be centered or that it will be perfectly spherical. The outside surface will be no smoother than the container. Power requirements would be high because of the need to heat the container.

4. Melted Wire or Tubing

It has been observed that a wire heated by resistance to a temperature above its melting point will bead up under surface tension forces and will in fact separate into a series of spheres. The size of the spheres is that which tends to minimize the surface area. It might be possible to cast hollow balls by starting with tubing which has been pinched off at appropriate intervals. This simple technique has uses and advantages similar to the detached sphere sting method. The problems include control of the sphere after melting. Furthermore, this technique also requires resistance rather than electron beam heating.

C. MATERIALS AND METHODS SELECTED FOR FURTHER INVESTIGATION

On the basis of this screening procedure, we selected 350T maraging steel, 440 stainless steel, Astralloy, Star J Stellite, aluminum-4 1/2% copper alloy, nickel-12% tin alloy, and pure nickel for further investigation. We concluded that the forming spheres on stings using the captive sphere or nonwetting dissimilar materials approach would be the most desirable casting method. Casting in a viscous melt was considered an alternative technique to simulate free float conditions.

VI. LABORATORY STUDIES

Problems associated with solidification shrinkage, non-uniform heating and cooling, and the small and finite mechanical forces acting on a solidifying mass, are likely to exert adverse effects on the characteristics of the casting, particularly its surface roughness and sphericity, even in zero-g. Furthermore, no experiment performed on earth can fully simulate either the conditions in an orbiting spacecraft or the actual results of materials processing therein. However, laboratory experiments can demonstrate some of the problems which might occur in the orbiting laboratory and indicate which metals and alloys appear to offer the greatest potential for successful casting in space. Therefore, we conducted four types of experiments:

- Melting and casting of spheres held captive on stings or dropped through a 4-foot "shot tower".
- Melting of samples with a prototype electron beam gun.
- Measurement of vapor pressure of selected materials.
- Casting of metals in molten glass.

We performed these experiments on the following materials: Al-4 1/2% Cu alloy, Ni-12% Sn alloy, low alloy steel - "Astralloy", 350T high-tensile maraging steel, Co-Cr-Mo alloy-Star J Stellite, and type 440 stainless steel.

A. MELTING AND CASTING EXPERIMENTS

1. Apparatus and Method

A simple drop-tower (Figure 3) was constructed from clear quartz tubing. The upper end is a short length (about 6") of 1"-diameter quartz tubing. This section, which is surrounded by a "pancake" r.f. coil, houses the sample. The sample is held by a simple pin-vice; sample configurations are shown in Figure 4.

The lower end of the drop tower was immersed in a bath of vacuum pump oil which provided a means of quenching the samples at the end of their fall and also provided a seal from the atmosphere. Prior to each experiment the entire system was flushed with argon via an inlet port provided for this purpose (see Figure 3). A slight positive argon flow was maintained during the experiments.

The experiments simply consisted of energizing the r.f. coil sufficiently to cause melting of the sample. Heating was either

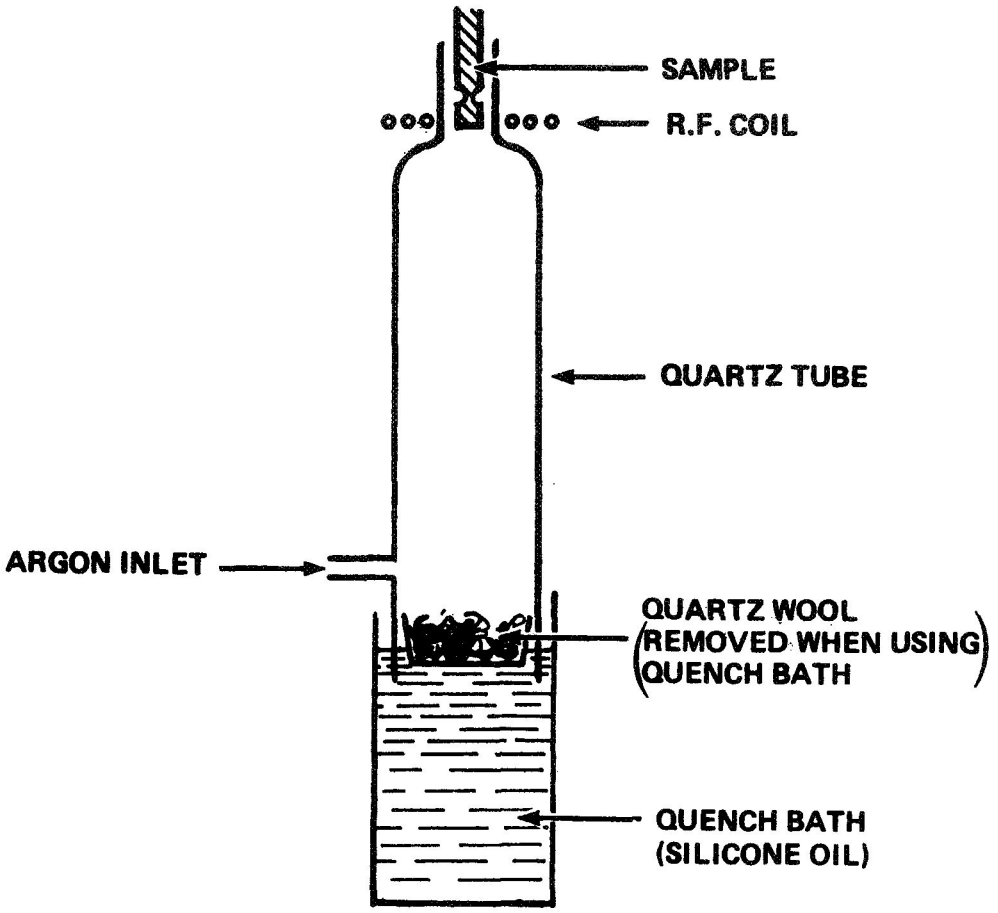

FIGURE 3 DROP CASTING APPARATUS

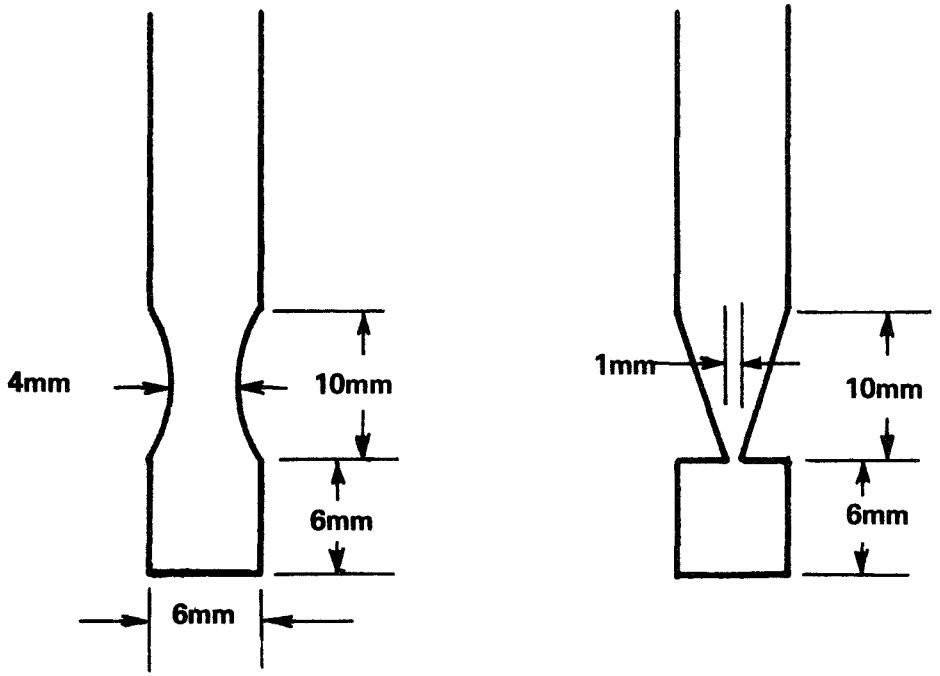

(a)
STING SAMPLE

(b)
DROP CASTING SAMPLE

FIGURE 4 STING AND DROP CASTING SAMPLE CONFIGURATIONS

discontinued, whereon the melt resolidified in situ, or continued until the molten section fell under gravity. Experiments were performed where the molten droplet was quenched directly into the oil bath and also where the droplet fell into a small dish of quartz wool floating on the surface of the oil bath (see Figure 3).

After each experiment the samples were removed from the apparatus, examined for sphericity and surface finish, and sectioned for metallographic examination.

2. Results

Aluminum-4 1/2% copper was the lowest-melting-point alloy investigated (M.P. 600°C). The drop casting experiment was unsuccessful because impact with the base of the apparatus occurred prior to freezing. Difficulty was also experienced during the captive sting experiment. A large fraction of the bar either became molten or approached the melting temperature, whereon extensive deformation occurred. Laboratory work directed at using this alloy in sphere casting experiments was discontinued.

Nickel-12% Tin was used as a "back-up" alloy for the Al-Cu alloy. It was prepared by direct melting 99.999% pure elemental components in a recrystallized alumina crucible and subsequently casting them in a permanent steel mold, resulting in a homogeneous casting.

No serious problems were encountered with either the drop casting or the captive sting experiment. Some shrinkage porosity was observed in the microstructure, but this was not surprising because the freezing range (≈150°C) of the alloy is large. Figure 5 shows low- and high-magnification photomicrographs of the Ni-Sn material. In Figure 5a, part of the curved surface of the drop-cast ball is shown. Sphericity was quite good but surface smoothness suffered slightly from the shrinkage associated with final freezing. The microstructure (Figure 5b) was as expected and consisted of primary Ni-rich dendrites (some coring) with a semicontinuous interdreditic eutectic. Some shrinkage porosity was also apparent in Figure 5b. In the as-cast condition the hardness of the Ni-12% Sn alloy was found to be R_c = 10.

Spheres of good sphericity and surface finish were obtained by drop casting Astralloy (supplied by the Vulcan Steel Company of Birmingham, Alabama). Wrinkling of the surface resulting from shrinkage during final freezing was observed in one region. Metallography revealed some internal shrinkage porosity. In the as-cast condition this alloy had a hardness of R_c = 34.

We subsequently attempted to increase the hardness by addition of extra crabon. As received, Astralloy contains 0.25% (nominal) of carbon. An additional 0.25% was added by melting a cylindrical Astralloy slug containing a blind hole into which the required

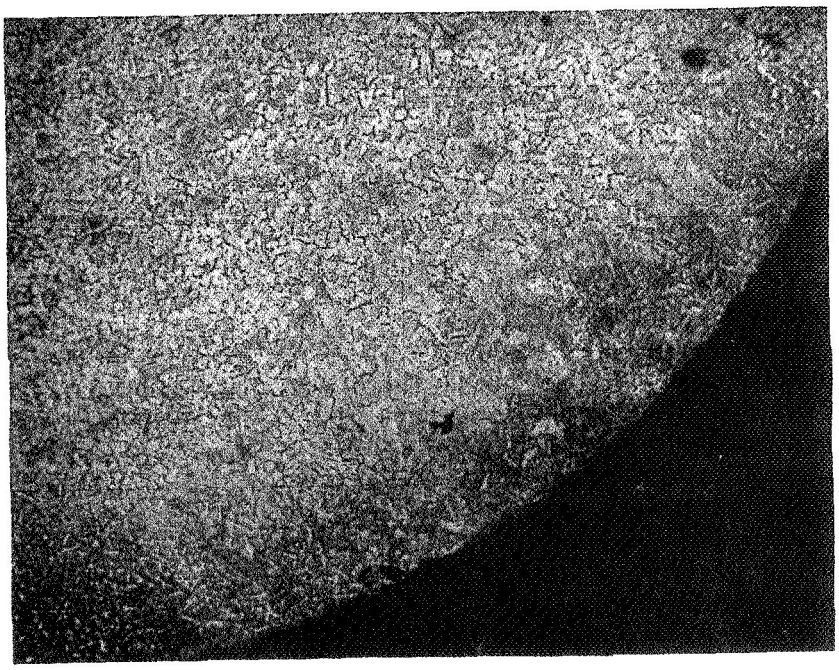

(a) MAG: X 62

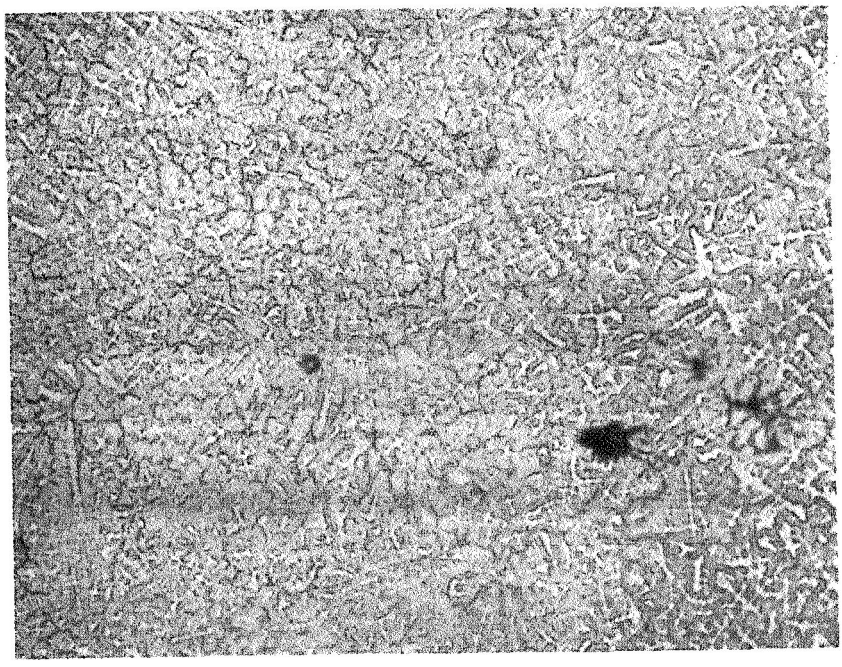

(b) MAG: X 225

FIGURE 5 MOSAIC PHOTOMICROGRAPH SHOWING STRUCTURE OF DROP CAST BALL OF Ni-12wt% Sn ALLOY

quantity of carbon was placed. A small, tight-fitting pin was driven into the hole, thereby preventing loss of the unalloyed carbon by oxidation. Melting was carried out under an argon atmosphere. The melt was held in a recrystallized alumina crucible. After melting, the alloy was cast in a small steel mold, thereby yielding 2-1/2" long x 1/4" diameter sticks.

Sphericity and surface smoothness were found to be similar to that obtained with the unmodified alloy. Difficulty was encountered during the metallography of the high-carbon material and the etching characteristics suggested that a large volume of retained austenite was present in the structure. Hardness measurements ($R_c < 10$) supported this viewpoint. In order to clarify the picture a Debye-Sherrer pattern was obtained (Cu-Ka radiation) and from these observations it was concluded that austenite is the predominant phase in the as-cast, high-carbon alloy. Figure 6 a and b are respectively low- and high-magnification photomicrographs of this alloy. Shrinkage porosity is clearly visible. The modified Astralloy material should respond well to heat treatment since the retained austenite will decompose via the autectoid reaction.

A sample of 350T high-tensile, maraging steel was obtained from Vasco Metals, Inc., Latrobe, Pennsylvania. The alloy was readily cast in both the drop and captive sting modes. Surface finish and sphericity were found to be similar to Astralloy. However, no internal shrinkage porosity was observed. As-cast, the hardness of this alloy was $R_c = 22\text{-}25$, but by using a suitable aging treatment the hardness could be significantly increased.

Figure 7 shows the microstructure of the maraging steel. Very large dendrites are clearly visible. The two photographs were obtained from the captive sting experiment with the top view showing the junction between the melted and unmelted (sting) portions. The bottom picture shows the curved surface of the melted and resolidified portion. It is clear from these photographs that freezing proceeds from both the outer (spherical shaped) surface and the solid (sting) liquid interface. The presence of a captive sting obviously influences the freezing pattern and, as a consequence, also influences the resulting microstructure, at least over a large region of castings prepared in this mode.

A sample of Star J Stellite (supplied by the Metals Division of Union Carbide, Inc.) was found to be the best overall material of all those we investigated. No internal shrinkage, surface wrinkling, or marked departures from sphericity were observed. The hardness was found to be $R_c = 61$.

Figures 8 and 9 are mosaic photomicrographs showing parts of the captive sting and drop castings respectively. As noted

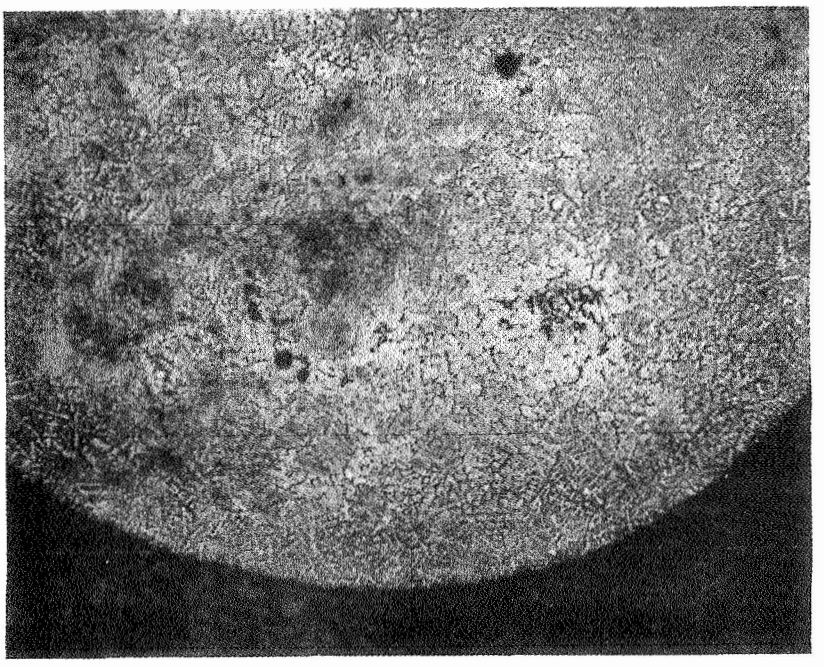

(a) MAG: X 62

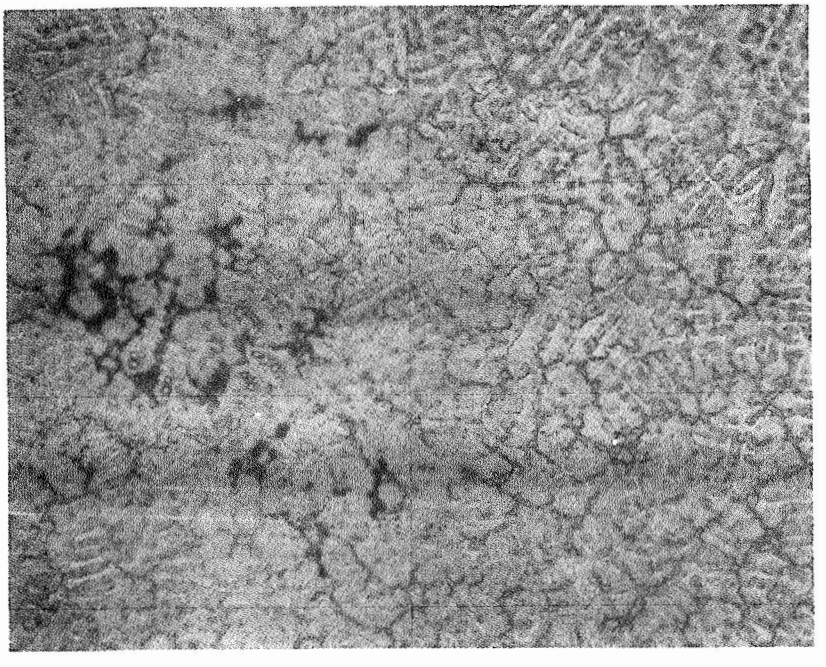

(b) MAG: X 225

FIGURE 6 MOSAIC PHOTOMICROGRAPH SHOWING STRUCTURE OF DROP CAST BALL OF MODIFIED ASTRALLOY

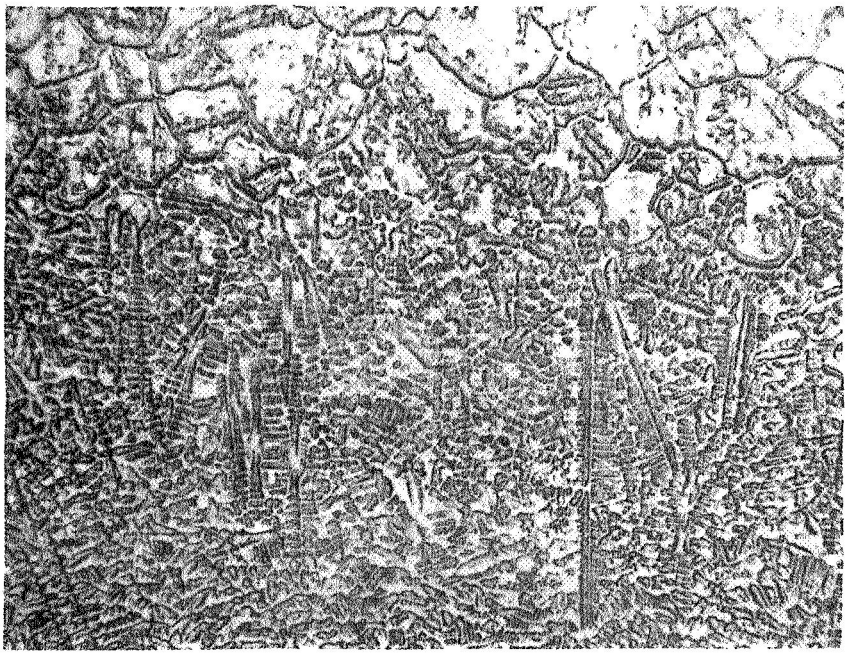

MAG: X 62

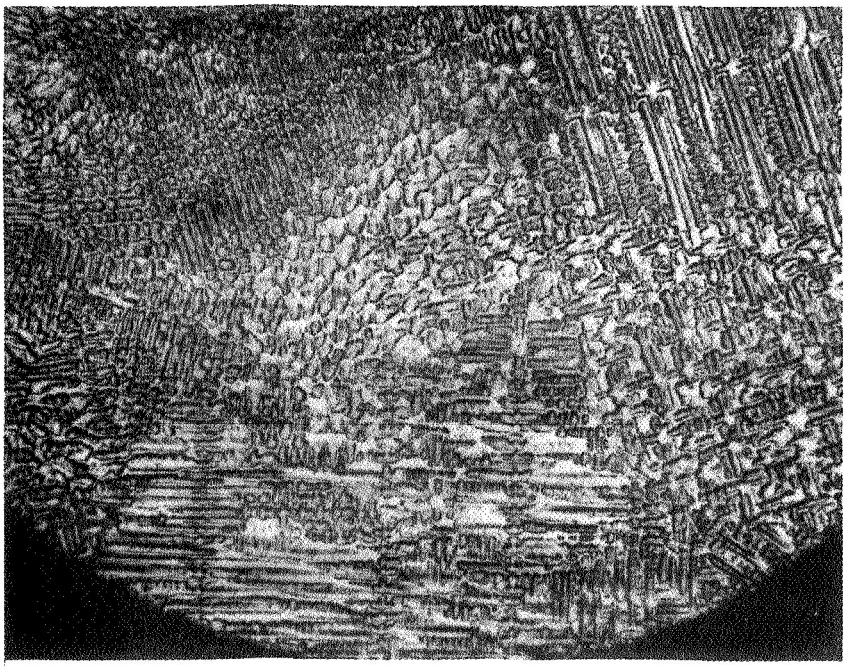

MAG: X 62

FIGURE 7 MOSAIC PHOTOMICROGRAPH SHOWING STRUCTURE OF CAPTIVE STING-MELTED 350-T MARAGING STEEL (NOTE DENDRITE ORIENTATION)

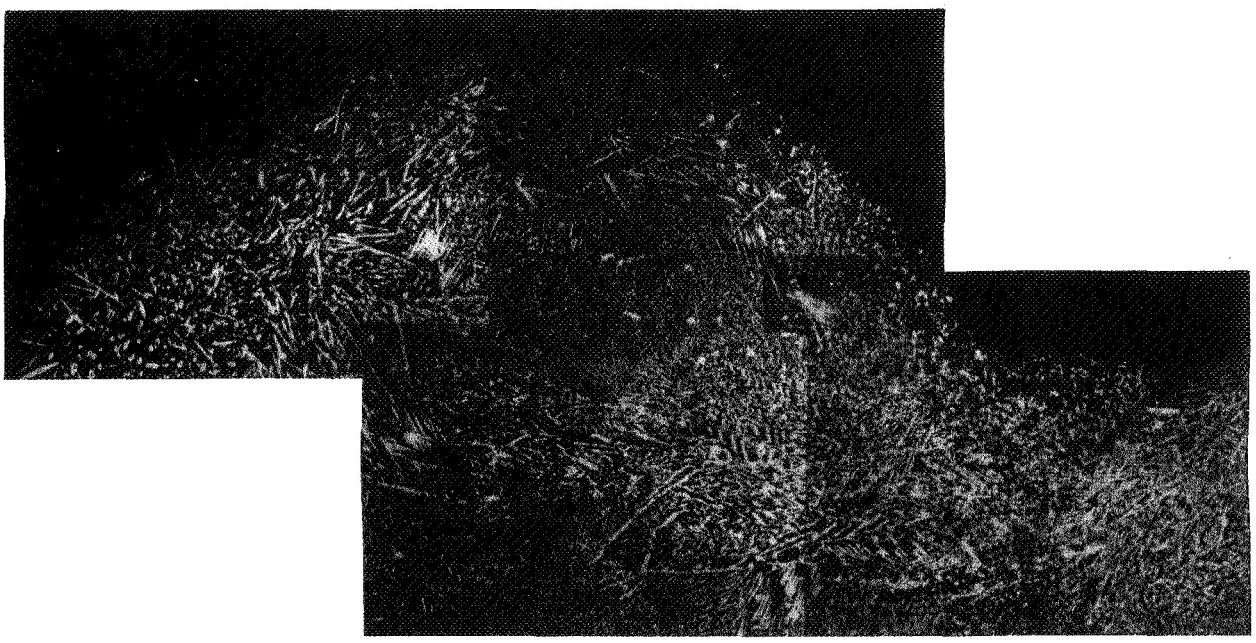

MAG: X 36

FIGURE 8 MOSAIC PHOTOMICROGRAPH OF CAPTIVE-STING MELT OF STAR "J" STELLITE

MAG: X 62

FIGURE 9 MOSAIC PHOTOMICROGRAPH SHOWING STRUCTURE OF A DROP CAST BALL OF STAR "J" STELLITE

with the maraging steel, the presence of a captive sting influences the microstructure. These effects are clearly visible in Figure 8, which shows the necked-down region of contact between the sting and the casting.

Examination of Figure 9 (drop cast ball) reveals that freezing proceeds as expected, i.e., from the outer surface. The dendrite size and the secondary arm spacing are far larger in the interior of the ball. These results suggest that the success experienced with this material is due in part to the rapid formation of a relatively strong, solid, spherical shell which is able to withstand the stresses accompanying complete freezing.

A sample of 440 stainless steel was melted with no difficulty. However, both sphericity and surface finish were very poor. We performed no further work on this material.

B. ELECTRON-BEAM MELTING TESTS

Since electron-beam heating is to be used for the in-flight experiment, several alloys (configuration as in Figure 4a) were subjected to melting in the electron-gun facility at NASA MSFC. Table 7 shows the electrical power and time required for melting. Quite obviously, the 2-kw "space gun" will be adequate for melting purposes. Metallographic examination of specimens melted in the MSFC equipment revealed no apparent differences from the structures obtained using the shot tower equipment at ADL.

TABLE 7

POWER AND TIME REQUIRED TO MELT SELECTED SAMPLES WITH AN ELECTRON BEAM

Material	Power to Melt kv	Power to Melt ma	Time to Melt (sec)
Astralloy	15	10	70
350T Maraging Steel	15	12	30
Ni-12% Sn	14	18	7
Star J Stellite	14.4	16	14

C. VAPOR PRESSURE EXPERIMENTS

Small samples of maraging steel, Star J Stellite, Ni-12% Sn and Cu-Pb were analyzed with a Nuclide Associates 12" radius, 60° sector, magnetic focusing high-temperature mass spectrometer. The samples were contained in a molybdenum Knudsen cell, lined with high-purity boron nitride. The vapor molecules effusing

from the Knudsen cell were collimated by a series of slits, ionized with an electron gun, and magnetically focused onto an electron multiplier for detection. The background pressure in the source chamber was about 10^{-6} torr, of the same order of magnitude as the anticipated ambient pressure in the AAP Space Facility. The purpose of the experiments was to check for the absence of highly volatile impurities and to assess the degree of sample vaporization under the planned experimental conditions. The cell and instruments were calibrated using silver, which is readily available in very high purity and whose vapor pressure as a function of temperature is accurately known.

The results of the measurements are summarized in Table 8, which shows the principal components of the alloys, their mole fraction, the measured vapor pressure at temperatures near the melting point, and a calculated value of the partial pressure of each component obtained from the product of the mole fraction and the vapor pressure of the pure metal (ideal solution law). The agreement between the measured and calculated pressures is very good. The vapor pressures of constituents of all samples are less than 10^{-5} atm at temperatures near the melting points. Most constituents will have vapor pressures less than 10^{-7} atm. Because the rates of vaporization are directly proportional to the vapor pressures, we expect that samples of these materials will have negligible vaporization losses in the brief periods during which they are molten. For example, the rate of loss of iron from maraging steel at its melting point is only about 3×10^{-5} gm/cm^2 sec. Thus we conclude that electron beam melting will not result in significant vaporization losses during the flight experiments.

D. THE METAL IN GLASS EXPERIMENTS

We conducted several preliminary experiments in which we simulated zero-g by melting a small sample of a metal in a molten glass. By using a high-viscosity glass, we hoped to obtain solidification of the melt before contact was made with the crucible walls.

A number of glass melts were made using the barium oxide-boron oxide system. From observations of the viscosity, we selected mixtures containing 85% and 95% of BaO. The glass was melted in recrystallized alumina crucibles contained in a graphite susceptor heated by induction. Small slugs of Ni and Ni-Cu alloy were introduced into the molten glasses and the power was switched off to facilitate complete freezing within the crucible.

The resulting casting was of very poor sphericity. Apparently, contact with the crucible base occurred prior to freezing, and, from our observations we conclude that this approach would be difficult to utilize in practice. For each alloy system a

TABLE 8

VAPOR PRESSURES OF SAMPLE COMPONENTS NEAR THE MELTING POINTS

Elemental Composition	Mole Fraction	Measured Vapor Pressure, atm (T = 1723°K)	Calculated Partial Pressure, atm (T = 1700°K)
Maraging Steel			
Fe	0.615	3.78×10^{-6}	3.37×10^{-6}
Co	0.205	5.15×10^{-7}	6.15×10^{-7}
Ni	0.092	2.42×10^{-7}	3.87×10^{-7}
Mo	0.088	$<10^{-12}$	
Star J Stellite			
Co	0.491	5.67×10^{-7}	14.7×10^{-7}
W	0.071	$<10^{-12}$	
Cr	0.376	1.64×10^{-6}	7.75×10^{-6}
Ni	0.027	9.05×10^{-8}	11.3×10^{-8}
Fe	0.035	Not observed	1.91×10^{-7}
		Measured Vapor Pressure, atm (T = 1673°K)	Calculated Partial Pressure, atm (T = 1700°K)
Ni-12wt% Sn (6.25 mole %)			
Ni		4.08×10^{-6}	4.16×10^{-6}
Sn		0.94×10^{-6}	1.58×10^{-6}
		Measured Vapor Pressure, atm	Calculated Partial Pressure, atm
Cu-Pb			
Pb		1.43×10^{-5} (1000°K)	1.51×10^{-5} (1000°K)
Cu		5.55×10^{-7} (1400°K)	11.3×10^{-7} (1400°K)

specific glass composition with a well defined viscosity would be required; therefore, no further consideration was given to this type of experiment.

E. MATERIALS RECOMMENDATIONS

As a result of these laboratory experiments, we selected four materials for the flight experiments. In order of preference these are:

(1) Star J Stellite

(2) 350T Maraging Steel

(3) Ni-12% Sn

(4) Ni

(5) Astralloy (alternate)

(6) Al-4 1/2% Cu (alternate)

The stellite appears to fulfill all of the major requirements and, as previously noted, is the only material which has provided a high hardness. The maraging steel casts extremely well and the mechanical properties may be upgraded by heat treatment. Nickel-tin was found to yield acceptable castings although shrinkage porosity was evident. However, the longer freezing range alloys should be included in flight experiments because convection plays a significant role in the freezing of such materials on earth. The absence of these effects in zero-g could prove favorable both from the technological and scientific viewpoints. Nickel was selected (even though no experiments were conducted with the pure material) because of the potential for supercooling during free float conditions.

The low melting point Al-based alloy is less attractive because of the very long freezing times that would be required. Astralloy was considered an alternate because it did not yield spheres of hardness or sphericity as good as Star J Stellite or maraging steel.

VII. ANALYSIS OF EXPERIMENT PARAMETERS

Our preliminary heat transfer analyses, materials and methods screening, and laboratory studies indicated the desirability of conducting two types of sphere forming experiments: solidification with the molten spheres held captive on stings and solidification of molten spheres under "free float" conditions after detachment from stings. The following additional analyses were conducted to guide the design of hardware to implement these experiments:

- Estimation of the time for solidification and the uniformity of cooling of spheres of materials selected for flight experiments; and
- Evaluation of methods for removing spheres from stings.

A. TIME FOR MELTING, SOLIDIFICATION AND UNIFORMITY OF COOLING

Using the equations given in Part One, we estimated the melting solidification time for isolated 1/4-inch-diameter spheres of steel, nickel, and aluminum-copper alloys, as follows:

	Time (sec)	
Material	Melting at 2 kw	Solidification
Steel	< 3	18
Aluminum-Copper	1	426
Nickel	< 3	55

The melting times of these materials (and also Astralloy, Star J Stellite, and nickel-tin alloy) are well within the capabilities of the specified electron beam equipment. The solidification times for Astralloy and Star J Stellite will be similar to those of steel; nickel-tin alloy solidification times will be somewhat greater than the pure nickel, but much less than aluminum-copper. The Materials Melting Facility has a diameter of about 40 centimeters (16 inches). If a molten droplet were released with a zero separation velocity, the free-float time (t) would be: $t = (2\ell/a)^{1/2}$, where ℓ is the characteristic dimension and a is the residual acceleration of the chamber. If ℓ = 20 cm and $a = 10^{-4}g$, t would be about 20 seconds. If the residual acceleration were $10^{-5}g$, the maximum free float time would be about 64 seconds. Therefore, steel, Star J Stellite, Astralloy, nickel, and nickel-tin seem appropriate for use in "free float" as well as "captive sphere" solidification. In addition, any method used to separate the sphere from the sting should impart a

separation velocity less than 1/2 cm/sec to keep the molten sphere from impacting the chamber before it solidifies.

Table 9 shows the uniformity of cooling of these sample materials on stings, as given by the ratio of heat conducted along the sting to heat radiated from the surface. These estimates point out the necessity to reduce the sting diameter to less than 0.15 cm (1/16 inch) and preferably less than 0.05 cm (0.020 inch). The entire sting need not be this small, only that portion within about 1-1/4 cm (1/2 inch) from the sphere will be significant in establishing the temperature uniformity.

B. REMOVAL OF MOLTEN SPHERES FROM STINGS

We have considered several methods for removing a molten drop from a substrate so that it may remain in a free-float condition for a time long enough to permit its solidification before impacting the walls of the Metals Melting Facility. While the drop is still liquid, the principal factor determining its shape is the surface tension. We have assumed that typical values for surface tension of a molten metal are about 1000 to 1500 dynes/cm. Interfacial tension of the same order of magnitude was assumed to act at the boundary between the drop and the substrate if it is wetting or making a contact angle smaller than 90°. Cohesive energy for the molten metal was also assumed to be of the same order of magnitude. Internal forces resulting from the surface tension effects and cohesion must be overcome to attain physical separation of the molten sphere from the substrate by applying suitable external forces. Furthermore, the velocity with which the separation takes place must remain small to increase the "free float" time.

We examined three types of substrates: rods, foils, and tubes. We emphasized the analysis of tubes and rods because the case of a foil substrate is somewhat intermediate between the two but much less tractable.

A tube substrate would work as follows: When the metal sample in the tube is melted, two spherical surfaces will form as shown below.

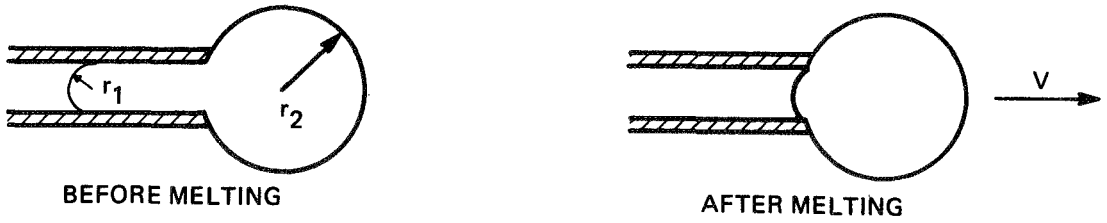

BEFORE MELTING AFTER MELTING

TABLE 9

RATIO OF HEAT CONDUCTED ALONG STING TO HEAT RADIATED FROM SPHERE SURFACE

Sphere Material	Sting Material	Sphere and Sting Diameters (cm) Sphere = 0.6 Sting = 0.1	Sphere = 0.6 Sting = 0.05
Nickel	Nickel	0.59	0.21
Nickel	Al_2O_3	0.27	0.09
Al_2Cu-Al	Al_2Cu-Al	2.3	0.8
Al_2Cu-Al	Graphite	4.2	1.4
Steel	Steel	0.36	0.12

If the radius $r_2 > r_1$, the external sphere will grow, since the pressure in the liquid resulting from surface tension is inversely proportional to the radius, ($Pi = 2\gamma/r$) and the final stage shown above will be reached. Then the drop will remain hanging at the orifice of the tube, attached to it by the adhesive force resulting from interfacial tension and Van derWaals force, unless (1) sufficient momentum is attained during melting to remove the sphere from the tube, or (2) additional energy is applied to the molten sphere to remove it.

When a rod substrate is used, a molten drop will form at the end and remain attached to the rod by a force proportional to the circumference of the rod, if the melt wets the solid sting because the surface tension acts in a direction tangential to the interface as shown below:

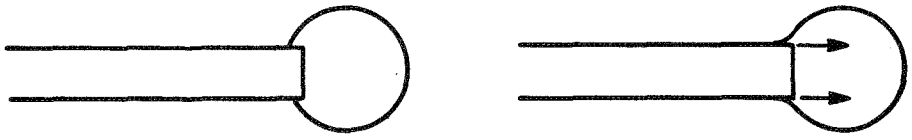

BEFORE MELTING AFTER MELTING

The drop may move along the rod if there are sufficient temperature gradients (due to the variation of surface tension with temperature) or by the reaction to the electron beam force. There is no a priori reason for the sphere to detach itself from the rod unless some external force is applied. If the rod is nonwetting, there is reason to believe that the drop will leave the rod because of the decrease in surface energy (if the nonwetting sting were indented into the sphere).

If a metal is melted using a foil as a substrate, a sphere will be formed resting on the substrate and making a contact angle with it in accordance with the interfacial tension, as shown below:

BEFORE MELTING AFTER MELTING

If the initial material is in a shape other than a sphere, a sphere will be formed. There is some evidence to suggest that the sphere may leave the nonwetting substrate because of the momentum acquired during the change of shape. As in the case of the sphere on a nonwetting tube or rod, movement of the sphere depends upon the viscosity, initial and final shape and size, and electrical effects.

We examined several types of forces which could be applied to free the drop from its substrate: gas pressure, inertial (impulse or oscillatory), centrifugal, electrostatic, electrodynamic, thermal (vaporization), self-removal (surface tension).

1. Gas Pressure

With a tubular substrate a gas pressure (inert gas) could be applied through the tube. For a nonwetting material (contact angle 90°) the pressure required to overcome the surface tension force is $2\gamma/a$ (a = radius of the tube). The pressure may be about 10^4 dynes/cm^2 (10 torr for a small tube (a = 0.2 cm). In practice, gas pressure would have to be increased until the drop was separated. Unless the supply of gas is stopped instantaneously, the flow of gas would impart to the free drop an initial velocity in excess of the permissible value.

2. Inertial Forces

Inertial forces may also be used to separate a drop from the substrate. If a rod is instantly accelerated away from the drop, a force (ma) can be generated equal or greater than the surface tension force. If the time required to separate the drop from the rod is Δt, the drop would be left with a velocity $v = a\Delta t$ toward the rod, which is undesirable. In order to leave the drop stationary in space, the motion of the rod should be programmed to first move forward with a constant velocity v_a and then moved backwards with the acceleration necessary for separation.

A practical way of separating the drop from the substrate by inertial forces is by exciting natural oscillations of the drop (e.g., by moving the rod or tube periodically in the axial direction). Since the viscosity of molten metal is low, resonance would be obtained with relatively small amplitudes of the substrate. The fundamental frequency of the dumbbell mode of a free drop is:

$$f_o = \frac{1}{\pi}\sqrt{\frac{2\gamma}{\rho r^3}} \qquad (10)$$

where ρ is the density of the drop. For r = 0.5 cm, the fundamental frequency is about 15 cycles/sec. The frequency of a

drop attached to a rod will be of the same order of magnitude, possibly somewhat higher. If the viscosity is small, separation of the two halves of an oscillating drop is found to occur when the maximum exceeds approximately two diameters of the original drop. If the viscosity is not small, a longer neck will have to be formed to achieve separation; and at high viscosities, the neck may extend indefinitely, without ever separating. In a practical experiment it may be difficult to drive the drop so that it leaves with little initial velocity.

3. Centrifugal Force

Centrifugal force may remove a drop of molten metal from a rod which it wets. Such a force would be obtained if the rod were arranged on a hub like a spoke of a wheel and set to rotate about an axis perpendicular to its length. The angular velocity of rotation necessary to overcome the surface tension force $2\pi\gamma r_1$ is found to be:

$$\omega = \sqrt{\frac{2\pi\gamma r_1}{mR}} \tag{11}$$

where r_1 is the radius of the rod, R the legnth of the rod from the axis of rotation to the center of the drop, m the mass of the drop, and γ the surface tension. The rotation speed in rps is $\omega/2\pi$, or, in rpm, 30 ω/π. Typically, for r_1 = 0.1 cm, R = 10 cm, m = 5 gms, and γ = 1000 dynes/cm, we obtain ω = 3.6 rad/sec, or 0.57 rps, or 34 rpm. Thus, if the drop can be rotated rapidly to achieve this speed, it can be removed.

4. Electrostatic Forces

Electrostatic forces have two effects on the molten drop. First, electrical charge on its surface tends to diminish the surface tension. If a drop of radius a is charged to a potential V, its surface is subject to a negative pressure, $P_e = -V^2/8\pi a^2$, while the surface tension generates a positive pressure, $p = 2\gamma/a$. This may be useful in reducing the overall magnitude of the surface effects. However, if $|p_e| \geq p$, it leads to instability of the kind which tends to break up the drop in smaller drops.

Secondly, a charged drop will be subject to an attractive (or repulsive) force in the electric field. If the potential of the drop is V (statvolts), its radius is r and the field intensity is E (statvolts cm^{-1}), the force is

$$f_e = rVE. \tag{12}$$

In order to make f_e comparable to the surface tension forces encountered, a potential of the order of 100 statvolts and field of the order of 100 statvolts/cm would be required. In practical units, this would be 30kv and 30kV/cm, respectively, which is high, but still feasible. In fact, potentials and fields of this magnitude may exist in the contemplated electron beam melting system and should be considered. Again, the force would remain acting on the drop after the separation is obtained and would accelerate it, unless the field is turned off at the moment of separation.

5. Electrodynamic Forces

Several problems could be avoided if instead of electron beam heating RF induction heating were adopted. A suitably shaped RF coil cannot only deliver the power necessary to heat and melt a piece of metal, but it can also confine it by means of electrodynamic forces to a small space near its center. This method is well known, theoretically understood, and used in various applications. The type of coil that produces a radial force on a piece of metal suspended in its middle is shown below:

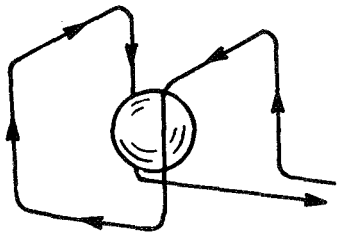

This is the same geometry as that used in the plasma containment apparatus used in the controlled thermonuclear fusion experiments (the "ALICE" experiment of UCRL).

A similar, but simpler, coil arrangement is suitable for suspending small molten spheres of metal at accelerations as large as the (terrestrial) g. Hence, the entire experimental set-up could be flight-tested in the laboratory. However, within the constraints of the initial orbiting laboratory, the use of electrodynamic forces is not feasible.

6. Electron Beam Force

The forces resulting from the impact of the electron beam on the drop of molten metal must also be considered. From

conservation of momentum and conservation of energy, we obtain, respectively

$$f = n\, m\, v^2\, A, \tag{13}$$

and

$$mv^2 = 2qV, \tag{14}$$

where n is the number of electrons per cm^3 of velocity v in the beam; q is the charge of electron, m its mass, and V the potential through which the electrons have been accelerated. Furthermore, the beam current is I = nqvA. From this, we obtain for the force acting over the area A

$$f = I\sqrt{2Vm/q} \tag{15}$$

For typical values, I = 0.1 amp (3 x 10^8 stat amp), V = 20,000 volts (67 stat volts), and q/m = 5.27 x 10^{17} statcoul/gm, we obtain f = 4.8 dynes. This force is small compared to the surface tension force on a 0.1-cm-diameter rod of about 300 dynes and would not be sufficient to remove it from the substrate.

7. Thermal Methods

A purely thermal method for separation of the drop from the rod was considered: if a relatively large drop is melted at the tip of a thin rod and another electron beam is focused at the neck and supplies enough heat to reach a temperature sufficient to evaporate the metal, separation may be achieved.

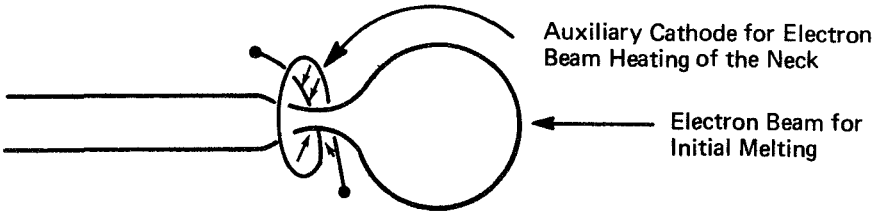

Experimental work at NASA MSFC has indicated that it is very difficult to vaporize sample materials rapidly enough to achieve separation. Also, a secondary electron beam source would be required.

8. Self-Removal Methods (Using Surface Tension)

a. Tube Substrate

We considered the dynamics of a drop of molten metal held by capillary forces in a tube of material which it does not wet, as shown below:

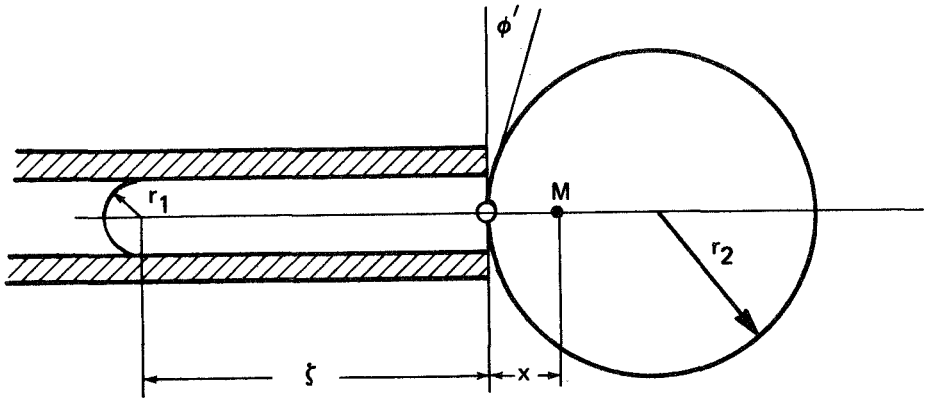

We assumed that the wetting angle ϕ' meets the condition $\cos \phi' > (r_1/r_2)\ (\gamma_s/\gamma_m)$, where γ_s is the interfacial tension between the tube material and vacuum, and γ_m is the interfacial tension between the molten metal and vacuum. Because of the difference in the radii r_1 and r_2, the entire mass of the molten metal will be subject to a force

$$f = 2\pi\gamma r_1^{\,2}\ (r_1^{\,-1} - r_2^{\,-1}) \tag{16}$$

driving it from left to right in the diagram. The center of mass M at x is accelerated and an equation of motion can be written describing the situation. Its solution is quite awkward. However, we can solve the simpler equation obtained if we assume that the radius of the tube is negligible compared with the radius of the drop ($r_1 << r_2$), a case of practical importance. Neglecting viscosity and friction effects, we obtain

$$\rho\ (\frac{2\pi}{3}\ r_1^{\,3} + \pi r_1^{\,2}\xi + \frac{4}{3}\ r_2^{\,3})\ \ddot{x} = 2\pi\gamma\ r_1. \tag{17}$$

If at $t = 0$, $x = 0$, and $\dot{x} = 0$, the final velocity of the center mass is approximately

$$v = \sqrt{\frac{3\gamma r_1}{\rho r_2^2}} \tag{18}$$

Typically, for $\gamma = 1000$ dynes/cm, $r = 0.1$ cm, $r_2 = 0.5$ cm, $\rho = 8$ gms cm^{-3}, a velocity of $v \approx 11$ cm sec^{-1} is calculated. If the total mass ($M = \rho V$) is taken to be about 5 gms, the kinetic energy of the mass of molten metal moving out of the tube is approximately 300 ergs. This appears to be adequate to overcome a potential barrier that may arise at the mouth of the tube from surface tension or adhesive forces.

b. Rod Substrate

We have also calculated the velocity of a sphere which is self-removed from a rodlike sting during electron beam melting, by relating the change in surface energy of the sphere-sting combination to the kinetic energy of the displaced sphere.

In the following diagram, b is the original radius of the sphere, and b' is the final radius of the sphere; the sting radius is a, and the sting itself is initially extended length ℓ into the sphere.

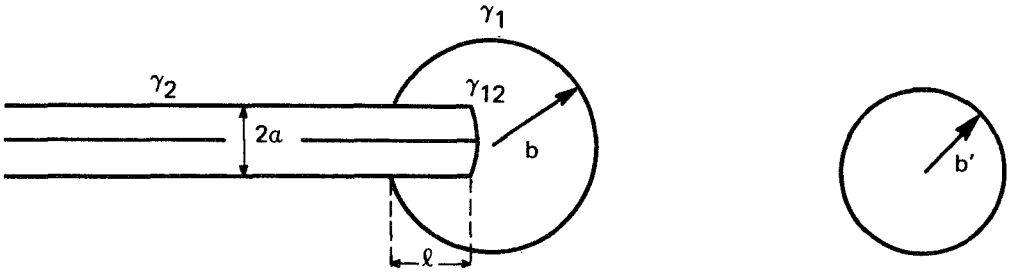

The total volume of sphere material is constant; therefore, the isolated sphere radius (radius after sting separation) is:

$$b' = b \left(1 - \frac{3}{4} \frac{a^2 \ell}{b^3}\right)^{1/3} \tag{19}$$

or approximately

$$b' = b \left(1 - \frac{1}{4} \frac{a^2 \ell}{b^3}\right) \tag{20}$$

Similarly:

$$b'^2 = b^2 \left(1 - \frac{1}{2} \frac{a^2 \ell}{b^3}\right) = b^2 - \frac{1}{2} \frac{a^2 \ell}{b} \tag{21}$$

The surface energy before sting-sphere separation is:

$$E = (4\pi b^2 - \pi a^2)\ \gamma_1 + (2\pi a \ell + \pi a^2)\ \gamma_{12} \tag{22}$$

where a, b, and ℓ are defined above, γ_1 is the surface tension of the sphere material, and γ_{12} is the sphere-sting interfacial tension. The energy after separation, E', is:

$$E' = 4\pi b'^2\ \gamma_1 + (2\pi a \ell + \pi a^2)\ \gamma_2 \tag{23}$$

where γ_2 is the surface tension of the sting.

The kinetic energy is the difference between E' and E:

$$\Delta E = -\pi \gamma_1\ (4b'^2 - 4b^2 + a^2) + \pi(\gamma_2 - \gamma_{12})\ (2a\ell + a^2) \tag{24}$$

Substituting for b'^2 gives:

$$\Delta E = -\pi \gamma_1 \left(-\frac{2a^2 \ell}{b} + a^2\right) + \pi(\gamma_2 - \gamma_{12})\ (2a\ell + a^2) \tag{25}$$

From a force balance at the interface

$$\gamma_2 - \gamma_{12} = -\gamma_1 \cos \phi \tag{26}$$

where ϕ is the contact angle of the sphere with the sting.

Combining these two equations:

$$\Delta E = \pi\gamma_1 a^2 \left[\left(\frac{2\ell}{b} - 1\right) + \cos\phi \left(\frac{2\ell}{a} + 1\right)\right] \tag{27}$$

For the specific case where the sting extends originally into the center of the sphere, that is, $\ell = b$, the kinetic energy equation simplifies to:

$$\Delta E = \pi\gamma_1 a^2 \left[(1 + \cos\phi) + \frac{2b}{a}\cos\phi\right] \tag{28}$$

If the angle at the interface is 90° ($\phi = 90°$), the cosine will be zero and the kinetic energy equation simplifies to:

$$\Delta E = \pi\gamma_1 a^2 \tag{29}$$

Thus, if ϕ were less than 90° (i.e., nonwetting) considerably more energy could be imparted to the sphere. For example, if $\cos\phi = 1/2$, the energy would be given by:

$$\Delta E = \pi\gamma_1 a^2 \left(\frac{3}{2} + \frac{b}{a}\right) \tag{30}$$

In any case once ΔE is calculated, the maximum velocity of the sphere is readily determined from:

$$v = \left(\frac{2\Delta E}{m}\right)^{1/2} \tag{31}$$

In this analysis we assumed that melting of the sphere is instantaneous and other effects (e.g., viscosity) which would reduce the sphere velocity below this maximum value are negligible.

We estimated velocities for spheres of nickel, aluminum, and steel. Table 10 shows the results for spheres of 0.6 cm (1/4 inch) initial diameter with different sting diameter and different sting insertion lengths. A 90° interface angle has been used in the calculations. The maximum velocities which could be obtained are quite high; however, viscosity and finite contact angle effects, as well as non-instantaneous melting, will make the actual velocities smaller. Laboratory experiments are required to confirm these analyses and to determine which materials could be used as nonwetting stings.

TABLE 10

VELOCITIES OF SELF-REMOVED NICKEL, ALUMINUM AND STEEL SPHERES (0.6-CM DIAMETER)

Material	Sting Radius (cm)	Initial Sting Insertion Length (cm)	Final Sphere Velocity (cm/sec)
Nickel:	0.03	0.3	2.33
	0.03	0.2	1.36
	0.06	0.3	4.89
	0.06	0.2	2.81
	0.10	0.3	9.06
	0.10	0.2	5.13
Aluminum:	0.03	0.3	3.10
	0.03	0.2	1.79
	0.06	0.3	6.19
	0.06	0.2	3.70
	0.10	0.3	11.93
	0.10	0.2	6.76
Steel:	0.03	0.3	1.80
	0.03	0.2	1.04
	0.06	0.3	3.74
	0.06	0.2	2.15
	0.10	0.3	6.93
	0.10	0.2	3.93

c. Foil Substrate

Similar forces and velocities can result from melting a cylinder on a nonwetting foil substrate. However, the equations of motion are more difficult to evaluate because the directionality of the forces is not immediately evident. However, it is clear that there will be a component of force in the direction away from the foil when the cylinder is melted. There will also be force tending to move the sphere along the foil as well, because of the probable lack of symmetry of heating. These observations have been confirmed by experiments at MSFC. Thus, by properly shaping the material to be melted and by adequate control of melting, self-removal may be possible. The molten sphere should be nonwetting on the foil, but provisions must be made for electrical contact with the substrate during heating. This could be accomplished using a ceramic-coated foil to which a cylindrical sample has been spot welded.

C. COMPARISON OF METHODS

Basically, two types of methods have been evaluated: those in which positive movement of the sphere can be obtained through applying external forces, and those which use body forces or the change in energy of the melting sphere to move the center of mass, thereby moving the sphere. The advantages of the gas pressure, inertial (vibration or impact) and centrifugal force methods are: (1) they can be arranged to result in positive movement of the sphere; (2) they can be controlled by the astronaut; (3) they will definitely work. Their disadvantages are: (1) they may require extensive astronaut manipulation; (2) they require additional equipment; and (3) they may result in a high initial velocity of the sphere which will negate the potential effects gained in "zero g". These methods can be successful if an a.c. electrodynamic coil is used to control the sphere after release by one of these mechanisms. However, the use of the coil also requires additional equipment and astronaut control. We do not feel that electrostatics alone will be successful in removing the spheres in the present experiment designs. Similarly, thermal methods will probably not work.

The self-removal methods seem to have the greatest potential from the viewpoint of no additional equipment required, no astronaut control required, and the possibility for achieving relatively small initial velocities. Their main drawback, however, is that their operation is marginal, in that performance depends critically on the melting characteristics, location of the beam, and the selection of nonwetting materials as components of the sphere support. They do, however, represent simple experiments which could be incorporated into the present experiment design with minimum difficulty. On this basis, we recommend using either a sample on a nonwetting ceramic sting (with a conducting lead wire) or a

cylindrical sample on a foil as shown below. The sample on a sting has advantages of mechanical strength, ease of positioning and the potential for being a valid experiment even if removal is not achieved. The cylindrical sample on foil has the advantage of possible use of electrostatic charge build-up to aid in separation.

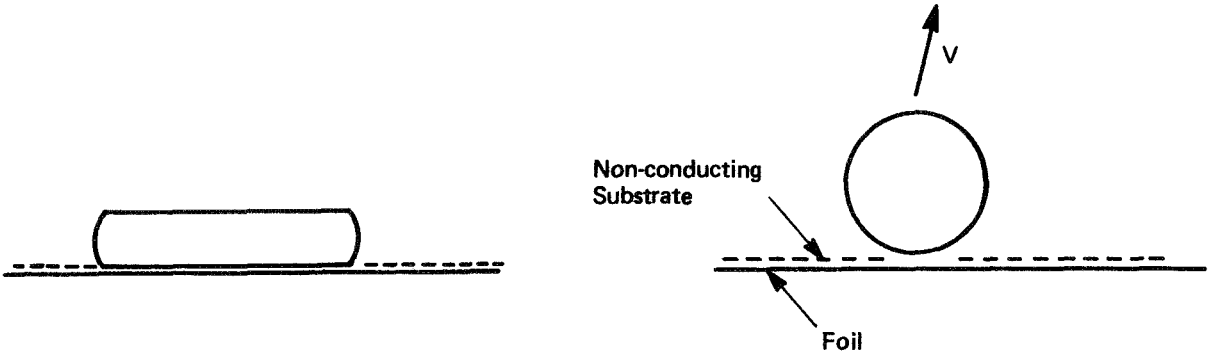

BEFORE MELTING

AFTER MELTING

BEFORE MELTING

AFTER MELTING

Additional laboratory studies are required to finalize the design of hardware to implement these methods.

VIII. PRELIMINARY HARDWARE DESIGN

A. DESIGN CRITERIA

The design of the spherical casting experiment is somewhat more complex than the composite casting experiment because of the requirements for movement of the samples and their positioning in the electron beam, control of heat transfer along the stings, removal from their support structure of the melted spheres with controlled acceleration, collection of samples, and storage of the samples and their support structure. The planned experiment hardware will consist of an experiment package, in which the samples to be melted and their supporting structure are stored outside the experimental chamber. The number of experiment packages will depend upon the available volume, weight, and power, the number of samples of each type selected for study, and the number of samples which can be mounted in a single support structure. The experiment package will be removed from its storage location by the astronaut, who will then remove its cover, and mount the package on the supports in the chamber.

This design is based upon our laboratory experiment program and analysis by which we established the following design criteria and principles:

1. Experiment Package

The principal function of the experiment package is to contain and store the sample materials and their support structure during all phases of the mission except when the experiment is being conducted. The materials and structural components must be chosen to meet the appropriate environment conditions.

Because it is necessary to position a number of samples in the electron beam, and because after the samples are melted and removed from their supports it is desirable to have as much open space as possible to provide increased "free float" time, the cover of the experiment package must be removed prior to emplacement of the experiment package in the vacuum chamber. Thus, a quick-release mechanism, giving positive clamping action to the cover, should be built into the experiment package enclosure.

The baseplate and sample-positioning mechanism should be as small as possible to reduce the potential impact area for the spheres.

2. Sample Holder

The sample holder must be designed to mate with the experiment package and the rotation (or movement) mechanism in the space

chamber. Because positioning of the sample will be important, the holder must be carefully aligned or keyed to prevent positioning errors.

The sample holder should hold and position at least 18 samples. The larger the number of samples, the greater the experiment reliability and the potential for gaining multiple data. Samples will be melted on stings; the sting should be an integral part of the sample holder assembly.

One concept for the sample holder is to have the samples form the spokes of a wheel, the hub of which is connected to the rotation and positioning mechanism. Positive electrical conduction paths must be assured in the sample holder design. The spacing of the samples must be sufficient to permit uniform cooling if they are retained on the stings. For samples which are to be removed from the stings, the projected cross-section of the remainder of the sample holder should be small to avoid contact. If possible, the samples should be arranged so that the net force applied by the electron beam should impart an acceleration opposite to the remainder of the equipment in the chamber. Similarly, the samples should be arranged in such an orientation that any residual acceleration of the spacecraft tends to move the molten samples away from the equipment, particularly the sting.

The sample holder and samples must be visible by the astronaut so that he can control the melting and shut off the electron beam when melting is complete.

For "captive sphere" experiments, the sting should be shaped to minimize heat conduction along its axis, as well as to retain the molten sample.

For samples which are to be "self-removed" after melting, there must be provisions for their positive mechanical and electrical attachment during melting; these stings and samples must also be chemically compatible.

After the experiment is performed, the sample holder should be detached from the positioning mechanism and stored outside the chamber in the original experiment package. Therefore, the package design should provide mechanical protection for the samples both before and after the experiment is performed.

3. Other Criteria

Molten samples should solidify before they reach the chamber wall to reduce the possibility of adherence.

The chamber vacuum line should have a screen or some other barrier to prevent the molten or solidified samples from entering the vacuum valve.

There should be radiation shield to prevent stray electron beam radiation from reaching the chamber walls.

Thermal radiation from hot samples, either on the stings, free floating, or at rest near the wall, must not cause local overheating of the chamber.

B. HARDWARE COMPONENTS AND EXPERIMENT OPERATION

We prepared preliminary engineering drawings of the hardware selected for the sphere casting experiment. (An artist's conception of the experiment is shown in Figure 1.) The experiment package is approximately 8 x 8 x 7 inches and consists of three major parts: a removable cover, a baseplate with a rotation and positioning mechanism, and a sample holder.

The cover, fabricated of fiberglass, aluminum, or some other lightweight material, completely surrounds the rotation and positioning mechanism and fits into a lip or groove in the baseplate. It is held in place with two retaining bolts. The bolts can be either a quick-release type, or removable with a tool. Holes are provided for evacuation, if required, of the experiment package.

The baseplate will probably be made of aluminum with lightening holes. Calfax fasteners can be used to attach the experiment package both outside and inside the Materials Melting Facility. Inside the facility, mating pins or other keying techniques can be used to insure correct alignment so the fasteners will accurately position the sample holder. The baseplate also contains an electrical connector. Attached to the baseplate is a lightweight motor support structure which will hold a motor or sample-positioning device. The most simple device would be an 18-position solenoid stepper (e.g., Rotonetic Solenoid Stepper, Heineman Electric Co., Trenton, N.J.). Each time the solenoid is pulsed, the sample holder would be rotated 20°. The positioning accuracy of such a device is sufficient to center the sample within the electron beam, assuming the sample diameter is 1/4 inch and the beam diameter is 3/8 inch. This type of rotary actuator is lightweight, simple and reliable. An alternative would be a standard rotary stepping motor which would require a multiplexer to give the desired rotation increment on command from outside the chamber. Either of these designs will result in the accurate positioning of the sample in the electron beam, a task which must be performed automatically, as it would be too difficult and time-consuming for the astronaut to perform remotely. A third alternative would be to use a motor and gear drive arrangement. In any case, however, the shaft of the device should be keyed to the sample holder.

The sample holder shown in Figure 1 has a disk-like center support (3-inch diameter) and 18 samples mounted on stings, each about

1-1/2 inches long. During storage, the sample holder is contained in the top of the experiment package cover and held in place by a partition and a vibration-isolating foam. When the astronaut is ready to perform the experiment, he removes the cover, then the partition (the partition is held in place by the cover retaining bolts), the outer foam layer that protects the samples and the fragile stings. Then he removes the sample holder and mates it with the shaft of the positioning motor. (Most likely he would already have installed the baseplate in the Materials Melting Facility.) The sample holder must be grounded to the experiment chamber, and this probably can be done by using the motor shaft as a ground (since the current in the electron beam is quite low). An alternative would be to have the astronaut attach a wire loop directly from the sample holder to the baseplate; because the sample holder rotates only once, a simple light-weight spiral wire will be sufficient. At the conclusion of the experiment, the entire package can be re-assembled for return to earth.

The final design of the stings must await additional laboratory tests at NASA-MSFC. Most likely they will be about 1-1/2 inches long, and about 1/16 to 1/8 inch in diameter. A possible arrangement is to use eight stings with the "captive sphere" technique and ten for the "self-detaching" sphere method. The first type of sting will most likely be made of the same metal as the sample. A small tapered-neck of about 0.020 to 0.040 inch diameter near the sample would be used to minimize conductive heat transfer along the sting. The second type of sting would most likely be a ceramic tube, with a conducting wire along its center, the wire providing the ground loop for the electron beam. This type of construction would be rather fragile; however, cladding can be used to strengthen the ceramic--except at the end where it contacts the sample.

In Figure 1 we have shown the samples as spheres; cylindrical samples 1/4 inch long and 1/4 inch in diameter would be equally useful and easier to fabricate.

In the performance of an experiment, the astronaut would index the stepping motor until the desired sample is in the electron beam path and then initiate the beam. He will either terminate the heating when the sample melts (captive sphere) or it will be self-terminating when the sample is released from the sting. Laboratory tests will provide accurate estimates of the heating time.

Several other hardware components should be included. A screen should be placed in the vacuum line to prevent any samples (or debris from other experiments) from reaching and fouling the valve seal; also to prevent the samples from being lost. Another screen might be advisable in front of the viewing window. Although little

effect is expected if the molten sample impacts the chamber, it would probably be undesirable to have it strike and adhere to the window. An electron beam absorber or shield should be used at an appropriate point in the chamber to intercept the energy that goes around the samples.

IX. REFERENCES FOR PART TWO

1. T. Z. Kattamis, R. Strachan, and M. C. Flemings: Solidification of Iron Base Alloys at Large Degrees of Undercooling. Interim Report, Contract No. DA-19-020-AMC-0231(X) Frankford Arsenal (Sept. 1964).

2. T. F. Boer and M. C. Flemings: Effect of Solidification Variables on the Structure of Aluminum Base Ingots. Interim Report Contract No. DA-19-020-ORD-5706(A), Frankford Arsenal (June 1965).

3. D. R. Poirier, R. F. Polich and M. C. Flemings: Development of Superior Steels for Precision Gyro Spin Bearings. Tech. Report No. ML-TDR-64-276, Air Force Materials Lab. (Aug. 1964).

4. Investigation of Solidification of High Strength Steel Castings. Interim Report Contract No. DA-19-020-ORD-5443(X), Casting and Solidification Sect., M.I.T. (Sept. 1963).

5. T. Z. Kattamis and M. C. Flemings: Dendrite Morphology Microsegregation and Homogenization of Low Alloy Steel. TRANS. AIME 233, (1965) 992-99.

6. F. C. Quigley and P. J. Ahearn: Homogenization of Steel Castings at 2500°F. TRANS. AFS 72, (1964) 813-17.

7. K. A. Jackson, J. D. Hunt, D. R. Uhlmann, and T. P. Seward III: On the Origin of the Equiaxed Zone in Castings. TRANS. AIME 236, (1966) 149-158.

8. G. S. Cole and G. F. Bolling: Augmented Natural Convection and Equiaxed Grain Structure in Casting. TRANS. AIME 236, (1966) 1366-1368.

9. T. F. Bower and M. C. Flemings: Formation of the Chill Zone in Ingot Solidification. TRANS. AIME 239, 216-219.

10. J. A. Spittle, G. W. Delamore, and R. W. Smith: The Transport of Solid in a Metallic Melt. TRANS. AIME 242, 1478-1479.

11. G. S. Cole and G. F. Bolling: The Synthetic Equiaxed Zone. TRANS. AIME 245, 725-734.

12. Bruce Chalmers: Principles of Solidification, John Wiley, New York (1964).

13. M. C. Flemings: Private Communication.

14. R. M. Brick, R. G. Gordon, and A. Phillips: Structure and Properties of Alloys. McGraw-Hill (1965).

15. Aerospace Structural Metals Handbook, Syracuse University Press.

16. Richard Henry, Vasco Corp.: Private Communication.

17. G. A. Roberts, J. C. Hamaker, Jr., and A. R. Johnson: Tool Steels, ASM 1962.

18. W. A. Glaeser: High Temperature Bearing Materials. ASM Metals Engineering Quarterly 7, No. 2, 53.

19. L. B. Sibley and C. M. Allen: Friction and Wear Behavior of Refractory Materials at High Sliding Velocities and Temperatures. WEAR 5, No. 5.

20. Survey of Materials for High Temperature Bearing and Sliding Applications. WEAR 7, No. 5.

21. J. L. Walker: The Influence of Large Amounts of Undercooling on the Grain Size of Nickel. Physical Chemistry of Process Metallurgy-Part 2. Interscience, New York (1961).

PART THREE

THE COMPOSITE CASTING EXPERIMENT

X. BACKGROUND

There are two general types of composites of current interest, the dispersed particle composites and the fiber reinforced composites. The two types impart increased strength to structural alloys in different ways. The dispersed particles are not load-bearing elements and do not contribute directly to the strength of alloys, but rather serve to inhibit grain boundary shear and migration and to pin dislocation tangles. To be effective, particles should be in the 50-100 Å size range with a spacing of about 1μ. In fiber reinforced composites, on the other hand, the fibers contribute directly to the strength of the composite (S) in accordance with the law of mixtures:

$$S = V_f \bar{S}_f^* + V_m S_{mf} \quad (V_f > V_{min}) \tag{32}$$

where V_f and V_m are the volume fractions of fiber and matrix, respectively, $\bar{S}_f^*$ is the average fracture stress of fibers in the matrix, and S_{mf} is the stress in the matrix at the same strain as the fiber. A fiber is a material with a length to diameter ratio greater than 10:1 and an effective diameter of less than 0.010 inch. The law of mixtures is approximately valid for both continuous filament reinforcement and discontinuous whisker reinforcement, provided that the fibers are aligned, well-bonded to the matrix, without being degraded by it, and that the volume fraction exceeds a minimum value, V_{min}, usually about 0.2.

Fiber composites have been produced by eutectic and monotectic solidification as well as by direct bonding between separately manufactured fiber and metallic matrices. Because the eutectic and monotectic composites have many other applications in addition to strengthening, and because their formation may be enhanced by zero-g, we have included them in our screening of candidate materials for the composite casting experiment.

XI. PRELIMINARY SCREENING OF MATERIALS AND METHODS

A. PARTICLE DISPERSED COMPOSITES

Particle dispersed composites are made by internal oxidation or carburization of alloys; by mixing, hot pressing, and extrusion of small particle size metals and oxides; and by coprecipitation and subsequent powder metallurgy (TD-Ni and TD-Nichrome). The attempts on earth to grow particle dispersed composites from the melt have led to agglomeration, and massive segregation of particles to the top or bottom of the melt. Agglomeration is probably the result of thermal convection, and the massive segregation is almost certainly due to gravity; therefore, melt forming or casting of particle dispersed composites should be far more successful in zero-g.

An experiment of practical significance would be to weld TD-Ni or TD-Ni-Cr in the Orbital Workshop. If agglomeration of the thoria particles were eliminated, an important contribution will have been made to a problem that has never really been solved satisfactorily on earth. This experiment may be conducted during the planned welding experiment.

Denver Research Institute has attempted to prepare dispersion-strengthened composites by casting of supersaturated oxide-metal melts. The work, plagued by agglomeration of the oxide particles and gravity separation of the dispersed phase, has never been formally published. We expect that this process would greatly benefit from the absence of gravity; however, experiments with TD-Ni could probably be conducted more easily.

B. FIBER-REINFORCED COMPOSITES

In the production of fiber-reinforced composites, the major problems have been alignment, bonding to the matrix, and chemical reaction between the fibers and the matrix. These problems are equally as critical in zero-g as on earth, and any fiber-matrix system selected for space fabrication must previously have been shown to be physically and chemically compatible on earth. Some aspects of composite forming processes should be improved in the absence of gravity, particularly when a molten metal is involved in the process. For filament (continuous fiber) reinforced composites, once the reinforcement is well-aligned, it should be possible to vacuum infiltrate a much longer filament bundle with molten metal in space, where only capillary and surface tension forces are operative, than on earth, where run-down and spill-down of the molten metal is a problem. This process would not work with Al-B composites, due to the degradation of boron filaments by molten aluminum, but it should be effective for composites of nickel-coated alumina filaments in

aluminum. However, the limited space available for the AAP Workshop experiments compels us to assign a low priority to vacuum infiltration experiments.

With whisker reinforcements, alignment is very much more difficult than with continuous fibers, and gravity separation during infiltration with molten metals is a well-recognized problem.[1]

1. Candidate Materials Systems

We believe that the materials used in this experiment should be restricted to metal-matrix composites. Resin-matrix composites are in such an advanced state of development that even if important improvements in properties were demonstrated in zero-g fabrication, it would be difficult to gain widespread acceptance in the industry. Ceramic-matrix composites, on the other hand, are in such a primitive state of development that there is still controversy over whether they are at all functional. Metal-matrix composites are attracting a fair amount of interest, although only Al-B is in commercial use.

To date, most work on metal-matrix composites has been done with model systems, and has been aimed at demonstrating that the principles of fiber reinforcement are sound. In view of this situation, it seems unlikely that a product brought back from space will be commercialized immediately, but we hope that the experiments will at least demonstrate the kinds of improvement in properties that can be expected in zero-g. Once the imagination of earth-bound manufacturers is stirred, important commercial applications can be expected to follow.

As discussed previously, the advantages of zero-g fabrication of fiber composites seems to be greatest for processes involving a liquid at some stage of manufacture. Examples of composites that have been fabricated by liquid infiltration methods are given in Table 11. Many more have been tried.

In our discussions with workers in the field, the materials systems that have generated greatest interest for zero-g fabrication are:

SiC whiskers in Mg-35% Al (MAG)

Al_2O_3 (sapphire) whiskers in Al or Aluminum alloys

SiC whiskers in Al

C whiskers in Al

TABLE 11

COMPOSITES FORMED BY LIQUID INFILTRATION

Matrix	Fiber	Reference
Cu	W	Kelly and Tyson[2] McDanels[3]
Cu-alloy	W	Petrasek[4]
Al	SiO_2	Whitney and Riley[5]
Ag Al Ni	Al_2O_3 Whiskers	Mehan[6]
Ag	Steel Mo	
Al	B_4C	Gotti[7]
Cu	WC	Rodney and Long[8]
Haynes 36	Al_2O_3 SiC	Mitron[9]
Ni Al	Al_2O_3 Whiskers	Melpar[10]
Ag	W Steel	Hoffmanner[11]
Cu	Ta	Ahmad[12]
Al-alloy	SiC Whiskers	Mitron[9]

2. Methods

a. Melting of a Prefabricated Composite

Nickel coated SiC (or Al_2O_3) whiskers can be magnetically aligned, mixed with magnesium-aluminum (or aluminum) powder, cold pressed, and vacuum degassed on earth. The composite could then be contained in a crucible and melted in the Materials Melting Facility with an exothermal heater. This experiment should demonstrate that melting is feasible without fiber segregation or agglomeration. If the composite could be heated on a sting, released, and cooled in a free floating state, large supercooling is possible and segregation of the fiber to grain boundaries may be eliminated. However, the latter method is probably not feasible in the initial program.

b. Composite Fabrication in Zero-G

A more complicated experiment would involve magnetic alignment in space of the nickel-coated SiC or Al_2O_3 fibers contained within a tube, followed by partial immersion of the end of tube in an Mg-35% Al or Al melt to bring about vacuum infiltration. This would require considerable astronaut manipulation and probably not be possible in the first Orbital Workshop.

C. MONOTECTIC COMPOSITES

1. Candidate Materials

A monotectic point is an invariant of a binary system where two liquids (usually of different density) and a solid are in equilibrium. Considering binary metal systems alone, more than one hundred have monotectic behavior. One of the most intensively studied monotectic systems is Cu-Pb. The phase diagram in Figure 10 shows that at 954°C a copper-rich melt containing 14.7 atomic % Pb is in equilibrium with a lead-rich melt and solid copper. Above 1000°C, a Cu-50% Pb composition forms a single homogeneous liquid. Below this temperature the alloy separates into two liquids, and, as shown in Figure 11, gravity causes the Pb-rich liquid to sink to the bottom of the crucible. Solidification involves formation of solid copper and enrichment of the liquid between the dendrites with lead. Finally, as cooling proceeds, the lead melt rejects dendrites of copper until it freezes as pure lead at 327°C. Under zero-g conditions, massive segregation of the lead and copper-rich liquids cannot take place, and a very different structure must result on solidification.

Directional solidification of monotectics, like the directional solidification of eutectics discussed below, can give rise to rod composites. Livingston[13] has directionally solidified a

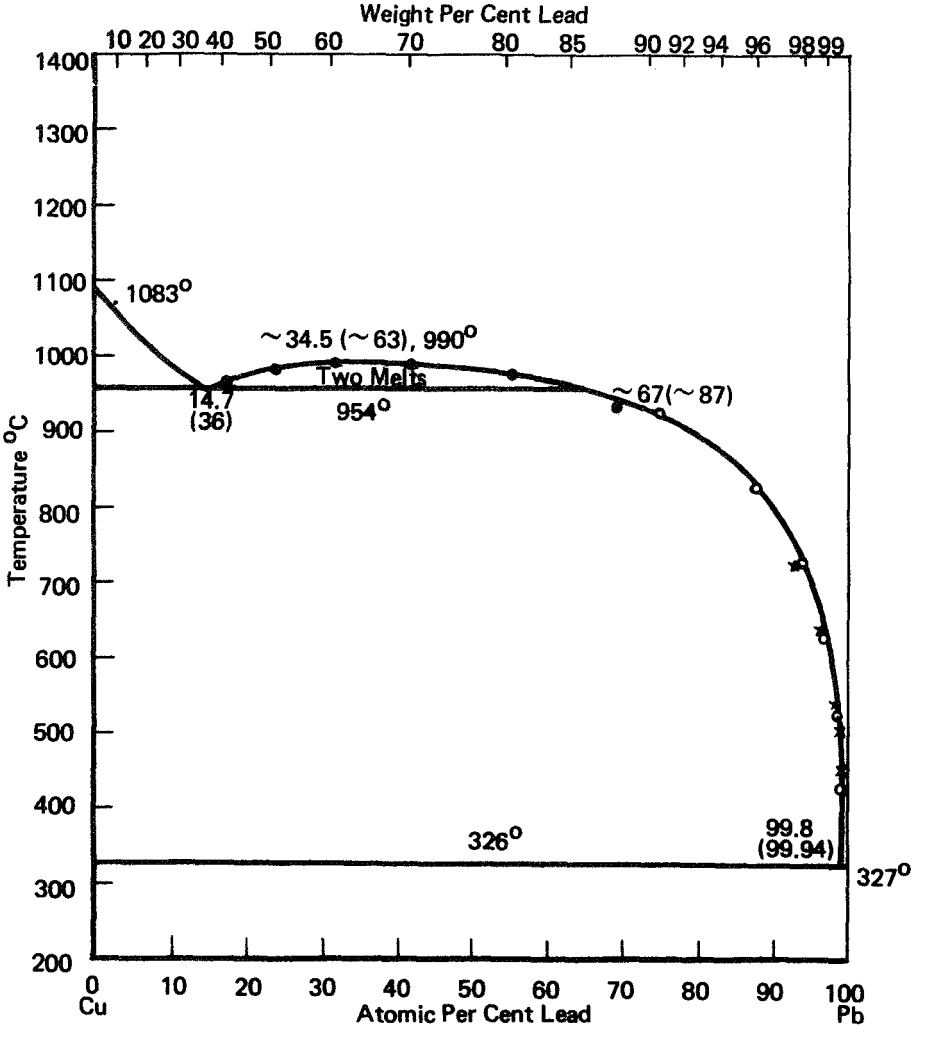

FIGURE 10 COPPER-LEAD PHASE DIAGRAM

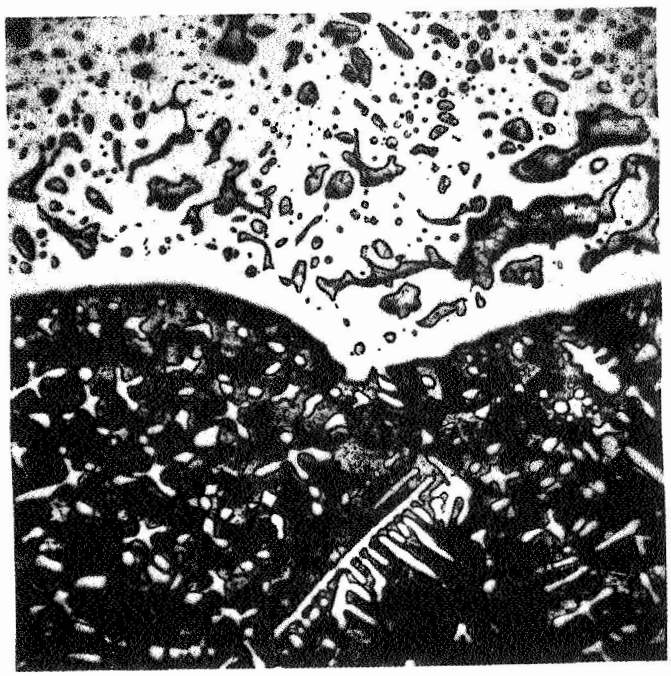

FIGURE 11 MICROSTRUCTURE OF Cu–50% Pb ALLOY

number of Cu-Pb alloys within the range of liquid-liquid immiscibility, and although he was troubled with gravity separation at the higher lead compositions, he was able to produce continuous filaments of Pb within a copper matrix. In comparing his experiences with directional solidification of eutectics and monotectics, Livingston indicated that the filaments or rods tend to be coarser with the monotectics. The inter-rod or inter-lamellar spacing, λ, is generally related to the growth rate, R, as follows:

$$\lambda^2 R = \text{constant} \tag{33}$$

The higher degree of supercooling possible in zero-g may permit an increase in R and consequent decrease in λ.

None of the monotectic systems we have considered appears to be of interest for strengthening applications. However, Livingston investigated Cu-Pb for its anisotropic superconducting behavior, and he indicated that he did get interesting effects, although he was not at liberty to disclose the details.

A monotectic system that might have considerable potential for superconducting applications is Nb_3Sn-Sn. The phase diagram shown in Figure 12 indicates that it is possible that directional solidification from compositions in the two-liquid region will result in long continuous rods of tin in a Nb_3Sn matrix. The material could be of interest in itself as an isotropic superconductor, or could possibly be treated to remove the tin, leaving long continuous filaments of Nb_3Sn. Whether the tin-rich liquid will elongate in the growth direction or nucleate on the Nb_3Sn solid as isolated droplets depends on the relative surface energies between $Nb_3Sn(S_1)$ and the Nb-rich liquid (L_2), the two liquids, and Nb_3Sn and the tin-rich liquid (L_1). According to the criteria developed by Chadwick,[14] isolated droplets will result if:

$$\gamma_{S_1 - L_2} > \gamma_{L_1-L_2} + \gamma_{S_1-L_1} \tag{34}$$

Elongated rods result if:

$$\gamma_{S_1-L_2} < \gamma_{L_1-L_2} + \gamma_{S_1-L_1} \tag{35}$$

and

$$\gamma_{S_1-L_1} < \gamma_{L_1-L_2} + \gamma_{S_1-L_2} \tag{36}$$

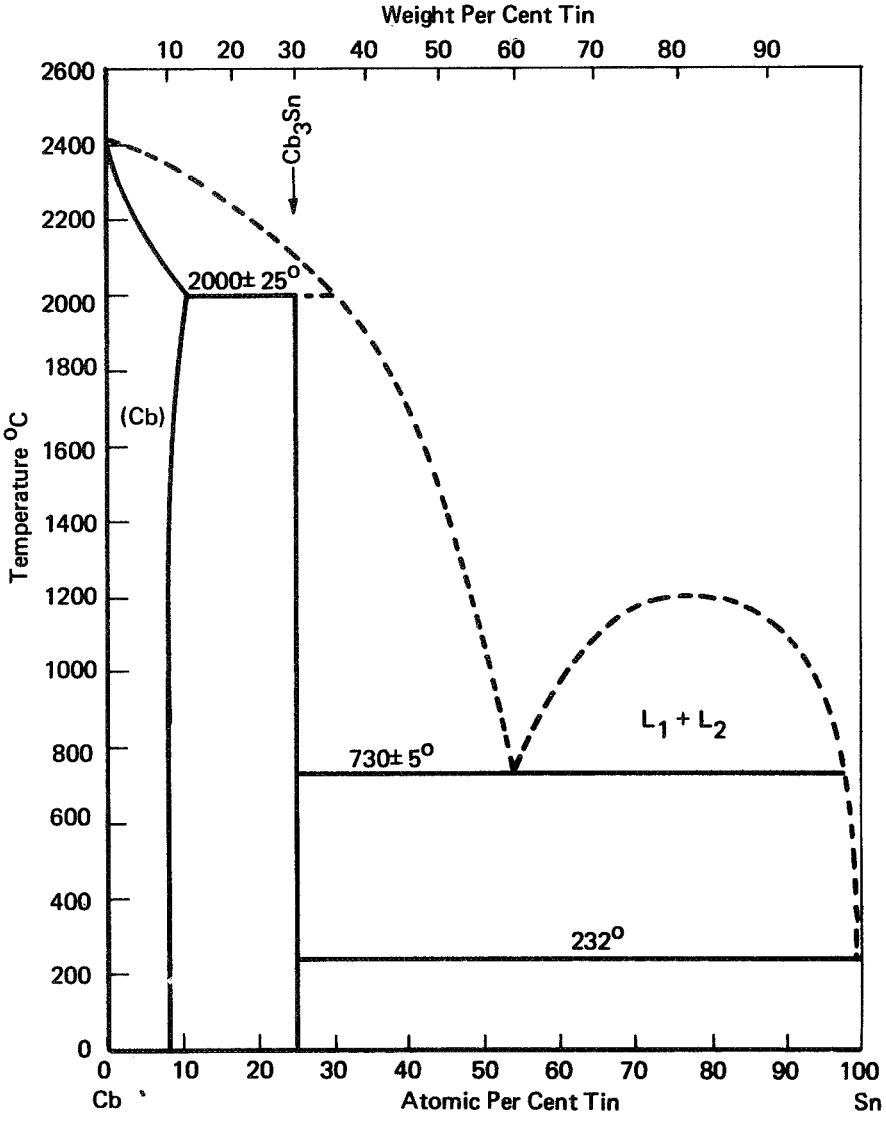

FIGURE 12 COLUMBIUM-TIN PHASE DIAGRAM

Since reliable surface tension data are not readily available, the behavior of the system can best be assessed by performing the directional solidification in the earthbound laboratory. While longer, thinner, straighter rods, with fewer branches or terminations, might be expected under zero-g conditions, the rod versus droplet formation should be independent of gravity.

If Nb_3Sn-Sn does not give a rod-like structure on directional solidification, Bi-Bi_2Se_3 can be considered as an alternative. This system is known to directionally solidify as Se rods within a single crystal Bi_2Se_3 matrix. Like the eutectic Bi_2Te_3-Te, the selenium system could be interesting for anisotropy of thermoelectric power and thermal and electrical conductivity, particularly if zero-g fabrication reduces the number of rod terminations.

2. Methods

a. Ingot Casting of Cu-Pb

A 50-50 Cu-Pb mixture could be heated in a graphite mold to a temperature slightly above 1000°C, where a single liquid phase exists. The electron beam or exothermic heater can be used. Since diffusion in liquids is rapid, the alloy should become well homogenized within minutes. The heater can then be turned off, and the melt allowed to solidify. As indicated in Figure 11, this experiment on earth leads to liquid-liquid separation due to gravity. In the zero-g environment there will be no separation, although the structure of the casting is otherwise difficult to predict. The comparison between a photomicrograph of a vertical cross-section of the casting fabricated in zero-g and the photomicrograph of Figure 11 should provide a very striking illustration of how gravity can affect solidification behavior. The experiment is not without practical utility, since Cu-Pb is used as a bearing alloy. To circumvent gravity separation in the two-liquid region, the alloys are now prepared by infiltration of porous copper with molten lead. The melt fabrication process in zero-g should produce a much better structure.

b. Directional Solidification of Nb_3Sn-Sn, Bi_2Se_3-Se, or Al-In

A mixture of Nb and Sn of the monotectic composition (54 atomic % Sn) could be heated above 800°C to bring about homogenization and then directionally solidified. The Nb-Sn mixture can be contained in a boron nitride spherical or cylindrical mold heated with an exotherm surrounding the mold. Heat would be removed directionally by means of a tungsten heat leak. After the Nb-Sn charge melts, it should be cooled slowly to form a composite of Sn and Nb_3Sn.

An alternative to the Nb_3Sn-Sn system is the Bi_2Se_3-Se system. The monotectic temperature is 618°C. The temperature at which the two liquids become miscible has not been identified, but should be suitable for the exothermal heaters. The same type of directional solidification apparatus could be used. Another alternative is directional solidification of Al-In. This monotectic is quite simple, there being no terminal solid solubility at either end of the constitutional diagram. Again, the same directional solidification method could be used.

D. EUTECTIC COMPOSITES

1. Candidate Materials

Directional solidification of eutectics gives rise to lamellar or rod-like composites. A lamellar structure generally results if the relative volumes of the two phases are approximately equal, and rod, needle or whisker composites result if one phase is present in much greater volume fraction than the other. United Aircraft has reported a number of eutectic systems that show improved strength characteristics compared to the pure metal. (See Table 12.) Dr. M. J. Salkind, of the Sikorsky Division of United Aircraft, indicated that none of the systems listed is under active commercial development. At least one eutectic system (not listed) has reached the development stage, but United Aircraft regards all details, including the systems, as proprietary. Since the primary aim of the eutectic melting experiments of this program is to demonstrate that, in the absence of thermal convection, more perfect composite structures will result, the most reasonable system to examine is $CuAl_2$-Al. The eutectic temperature is low, the $CuAl_2$ lamellae do strengthen aluminum, and a great deal of background information is available. Figure 13 is a photomicrograph of a directionally solidified $CuAl_2$-Al eutectic fabricated on earth. Termination faults are clearly in evidence, and we think these might be eliminated in a zero-g fabrication procedure.

While fiber composites have been investigated primarily for high strength, eutectic composites have been explored for many other applications in optics, electronics, and magnetics. Galasso[15] has reviewed some of the more interesting systems summarized in Table 13. The anisotropic properties of the thermoelectric eutectics can be advantageous in electronic applications. NiSb-InSb exhibits a very large magnetoresistive effect, and all of the eutectics based on InSb can be used as infrared polarizers. The superconducting eutectics have been difficult to prepare and have not really been characterized sufficiently to assess their ultimate potential. The optical eutectics must be transparent to take full advantage of their anisotropic properties. This has been difficult, partly because of oxide contamination[15] and possibly because of imperfections in structure. The ferromagnetic eutectics, characterized by

TABLE 12

EUTECTIC STRUCTURES WITH HIGH STRENGTH

System	Eutectic Temperature
Al_3Ni-Ni	1385°C
$CuAl_2$-Al	548
Ta_2C-Ta	2800
Cb_2C-Cb	2335
BeNi-Ni	1157
MoNi-Ni	1315

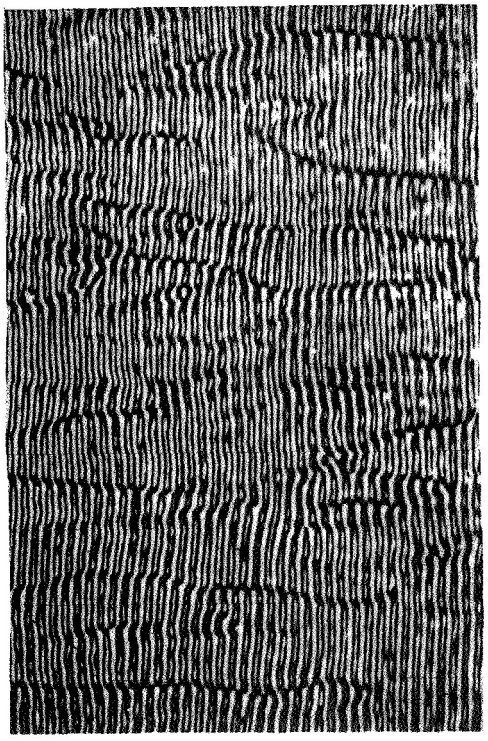

FIGURE 13 PHOTOMICROGRAPH OF UNIDIRECTIONALLY SOLIDIFIED Al–$CuAl_2$

TABLE 13

EUTECTIC COMPOSITES FOR OPTICAL, ELECTRONIC AND MAGNETIC APPLICATIONS

THERMOELECTRIC EUTECTICS

System	Reference
InSb-Sb	Liebmann and Miller[16]
Bi_2Te_3-Te	Galasso and Darby[15]

MAGNETORESISTIVE AND INFRARED POLARIZING EUTECTICS

System	Reference
NiSb-InSb	Weiss and Wilhelm[17]
CrSb-InSb	Paul, Weiss, and Wilhelm[18]
MnSb-InSb	Paul, Weiss, and Wilhelm[18]
FeSb-InSb	Paul, Weiss, and Wilhelm[18]

SUPERCONDUCTING EUTECTICS

System	Reference
Pb-4 atom % Ag	Levy, Kim, and Kraft[19]
Pb-74 Sn	Levy, Kim, and Kraft[19]
Pb-17.5 Sb	Levy, Kim, and Kraft[19]
Pb-28 Cd	Levy, Kim, and Kraft[19]
Sn-43 Bi	Levy, Kim, and Kraft[19]
Sn-33.5 Cd	Galasso[15]
Sn-15 Zn	Levy, Kim, and Kraft[19]
Bi-ϵ(Pb-Bi)	Levy, Kim, and Kraft[19]
Sb-Sb_2Tl_7	Levy, Kim, and Kraft[19]
β-InSn-γInSn	Levy, Kim, and Kraft[19]
In-$BiIn_2$	Levy, Kim, and Kraft[19]
Pb-$AuPb_2$	Levy, Kim, and Kraft[19]

TABLE 13 (cont'd)

OPTICAL EUTECTICS

System	Reference
NaF-LiF	Nichols[15]
$NaF-CaF_2$	Nichols[15]
$NaF-MgF_2$	Nichols[15]
$NaF-PbF_2$	Nichols[15]
$PbMoO_4-PbO$	Nichols[15]
CaF_2-NaF-LiF	Nichols[15]
LiF-NaCl	Loxham and Hellawell[20]
NaF-NaCl	Loxham and Hellawell[20]
NaF-NaBr	Loxham and Hellawell[20]
$ZnO-Zn_3Nb_2O_8$	Galasso[15]

FERROMAGNETIC EUTECTICS

System	Reference
Fe-FeS	Albright[21]
$Fe-Fe_xSb$	Galasso, Douglas, Batt, Darby & Tice[15]
$Co-Y_2Co_{17}$	Galasso, Douglas, Batt, Darby & Tice[15]
Co-CoSb	Galasso, Douglas, Batt, Darby & Tice[15]
$Ni-Ni_3Sn$	Galasso, Douglas, Batt, Darby & Tice[15]
$Ni-Ni_{15}Gd_2$	Galasso, Douglas, Batt, Darby & Tice[15]
$BaFe_{12}O_{19}-BaFe_2O_4$	Galasso, Douglas, Batt, Darby & Tice[15]

permanently magnetic rods or lamellae within a nonmagnetic matrix, show a hysteresis loop that is quite different from that obtained from the single phase magnetic material.

The use of controlled eutectics for nonstructural applications is still very much in its infancy. Hence, if real improvements in eutectic structure can be brought about in zero-g, the possibilities for space manufacture can be brought to the attention of the technical community before possibly more cumbersome methods of earthbound manufacture become firmly entrenched.

2. Methods

From this list of eutectics, four materials seem most promising. The $CuAl_2$-Al eutectic can be directionally solidified in a boron nitride mold similar to that used for monotectics. The eutectic, held in the ceramic crucible, is melted by an exothermic heater and allowed to cool under controlled temperature gradient conditions.

The Y-Co alloys are currently of great interest for their magnetic properties, and single-phase materials are being investigated by the Air Force Materials Laboratory. The Co-Y_2Co_{17} system melts at a somewhat higher temperature than the other systems we are considering. Therefore, modifications to the exotherm and crucible might be necessary to avoid undesirable chemical interactions.

InSb-Sb is a thermoelectric eutectic with a eutectic temperature of 500°C. It consists of Sb rods within an InSb matrix. It has been shown that the thermoelectric properties can be improved by reducing the rod size. Small rod size may be promoted in the zero-g environment, if, as we expect, higher growth rates can be sustained.

If Al_2O_3 whiskers are incorporated into the $CuAl_2$-Al eutectic composition, the whiskers should segregate to the $CuAl_2$ lamellae. This would produce a double composite system which could have higher strength than either the eutectic system alone or sapphire whisker reinforced aluminum.

E. RECOMMENDED MATERIALS FOR LABORATORY STUDIES

The composite experiments we selected for the laboratory program were:

- Ingot casting of 50-50 Cu-Pb
- Directional solidification of Nb_3Sn-Sn, with Al-In as a backup
- Directional solidification of $CuAl_2$-Al

- Directional solidification of Co-Y_2Co_{17}
- Directional solidification of InSb-Sb
- Directional solidification of Al_2O_3 whisker reinforced $CuAl_2$-Al
- Melting of an SiC-MAG or Al_2O_3-Al whisker reinforced composite
- Melting of TD-Ni or TD-Ni Cr

XII. LABORATORY STUDIES

We conducted three types of laboratory experiments to narrow our selection of materials and to provide data to facilitate the design of suitable exothermal heaters for the flight experiments:

- Directional solidification of Al-Al_2Cu, Pb-Sn, Nb_3Sn-Sn, InSb-Sb, $Co_{17}Y_2$-Co, Cu-Pb, and Al-In.
- Mixing SiC and Al_2O_3 whiskers in molten aluminum-based matrices.
- Melting TD-Ni and TD-Ni-Cr on stings.

A. DIRECTIONAL SOLIDIFICATION EXPERIMENTS

1. Apparatus and Method

The experimental arrangement used for directional solidification is shown in Figure 14. It consisted of a wire-wound furnace having an inner tube of 6" length x 1" diameter closed at one end. A small linear, axial temperature gradient exists in the furnace when electrical power is provided. The major temperature gradient "seen" by the sample is produced by means of a 1/4"-diameter tungsten rod held in contact with the upper surface of the melt. This tungsten rod is held at the other end in a water-cooled pin vice. The gradient can be changed by varying the water flow rate. The furnace is continuously flushed with argon.

The samples are contained in boron nitride crucibles of internal dimensions 2-1/4" long x 1/4" in diameter. Three blind longitudinal holes, of different length, are drilled into the crucible wall to facilitate thermocouple temperature measurements.

A typical experiment consisted of completely melting the sample, allowing the system to stabilize with a given water flow rate and finally decreasing the furnace power. The thermocouple signals were monitored continuously by means of a multi-channel recorder. Knowing the relative spacings of the hot junctions of the thermocouples allowed us to determine the axial temperature gradient. As the solid-liquid front passes each thermocouple a small thermal arrest occurs; from the time sequence of these arrests the approximate rate of solidification may be obtained. At the end of each experiment the samples were removed from the apparatus and subsequently sectioned for metallographic evaluation.

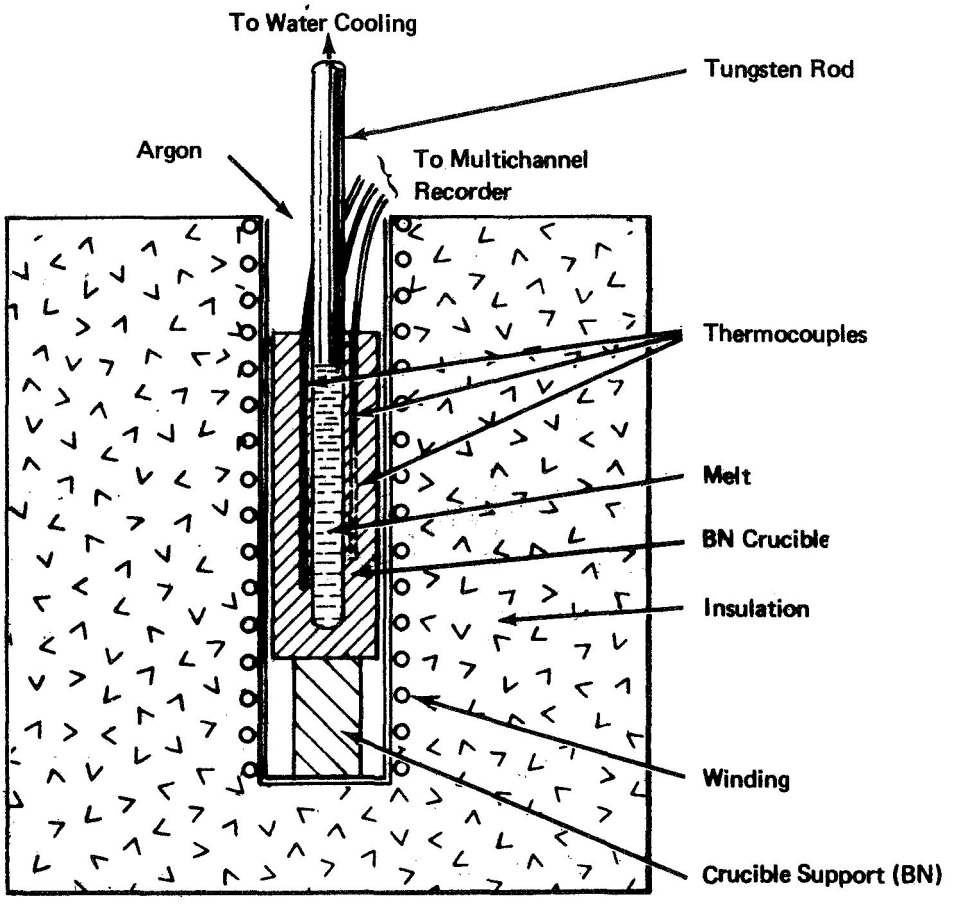

FIGURE 14 DIRECTIONAL FREEZING EQUIPMENT

2. Results

a. Pb-Cu

Figure 15 is a photomicrograph showing the structure obtained by chill casting a Pb-Cu alloy of the critical composition (63wt% Pb). The ingot was 2" in length and 1/4" in diameter. Because the thermal mass of the steel mole was very large compared to that of the melt, very rapid freezing was obtained. While the microstructure shown in Figure 14 is quite homogeneous (for a monotectic system) there is a gradation in the size of the copper phase (light colored), even with the rapid freezing rate obtained. This results directly from the density differences between Pb and Cu. The reason underlying the selection of the Pb-Cu system is that it could provide a simple demonstration of the potential benefit of zero-g. A relatively large mass of the alloy could be crucible melted and allowed to freeze in-situ. Massive phase separation in the orbital experiment should not occur. However, we feel that other materials will provide more scientific and practical information.

b. Al-Al_2Cu

This material was prepared by direct melting of the (99.999% pure) elements in a recrystallized alumina crucible under an atmosphere of argon. The melt was cast into a split steel mold yielding sticks of 2-1/4" long x 1/4" in diameter. The samples were inserted into a BN crucible containing three thermocouples embedded into the wall at different locations along the crucible length.

Figure 16 is a longitudinal section through a sample of Al-Al_2Cu eutectic alloy. The temperature gradient used was 23°C/cm and the approximate growth rate was 27 cm/hr. The rate determination is approximate only, since it is based upon the thermal arrests "sensed" by the three thermocouples. Some lag is to be expected by this technique since the thermocouples are positioned in the crucible walls.

No difficulties were experienced with the Al-Al_2Cu system. The fault density was found to be quite high (see Figure 16), but it would be most interesting to study any changes in fault density that may result from preparation in zero-g.

c. $Co_{17}Y_2$-Co

Great difficulty was experienced in preparing this alloy system. The melts were very turbulent and difficult to control. Even so-called high-purity yttrium contains dissolved gas (notably oxygen) which is released upon melting. Work on the Co-Y system was discontinued.

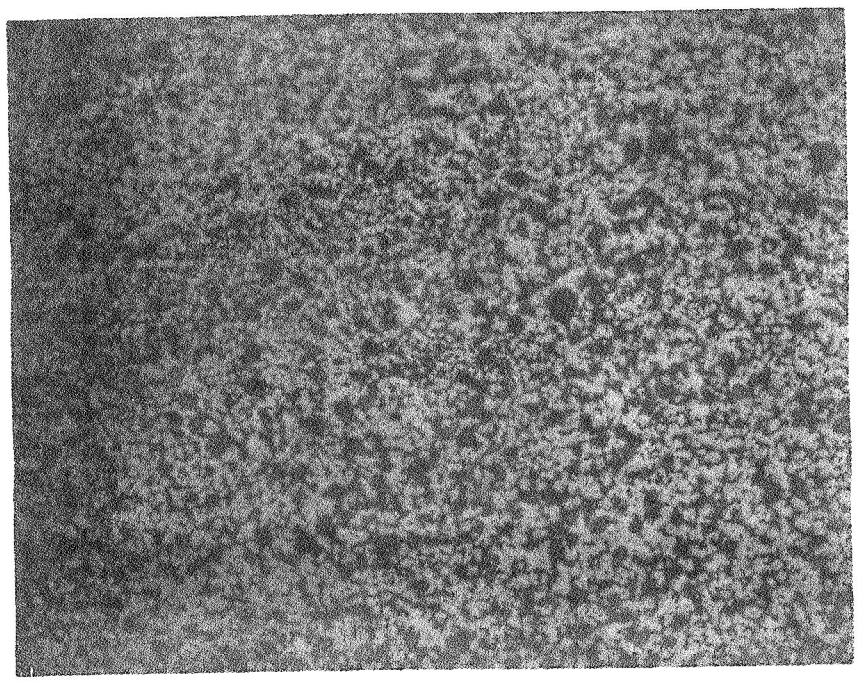

MAG: X 125

FIGURE 15 CHILL CAST SPECIMEN OF Cu-63% Pb ALLOY

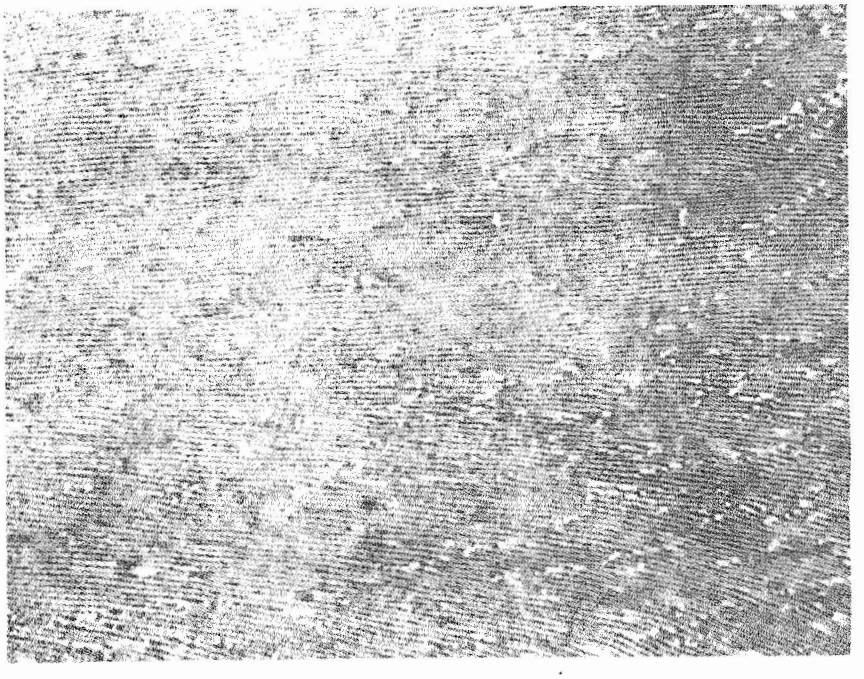

MAG: X 625

FIGURE 16 LONGITUDINAL SECTION OF Al-Al_2 Cu CONTROLLED EUTECTIC

d. InSb-Sb

This eutectic system, when prepared under high (200°C/cm) temperature gradient conditions, consists of triangular cross-sectioned rods of antimony aligned in a continuous InSb matrix. In the static experimental arrangement used, it is not feasible to attain such large gradients.

Figure 17 shows the type of micromorphology obtained under a gradient of 25°C/cm. The structure is lamellar with some tendency towards degeneracy. This system appears not to be a good candidate for the orbital experiments.

e. Nb_3Sn-Sn

The high reactivity of Nb made preparation of this system quite difficult in our relatively simple apparatus. As an alternative monotectic, we selected Al-In for further work.

f. Al-In

No experimental problems were encountered during directional freezing of the alloy. Figure 18 shows transverse and longitudinal sections of an ingot solidified at approximately 27 cm/hr under a temperature gradient of 23°C/cm (i.e., the same conditions used for the Al-Cu eutectic system). Figure 18 shows that there is a tendency for the In phase to form in a rod-like morphology. With the growth parameters used, it appears that the formation of a rod-like structure with this alloy system is marginal. Since gravity plays a very significant role in the freezing of monotectics, Al-In seems to be a very good candidate for the in-flight experiment.

g. Pb-Sn

This system is the lowest melting of any of the eutectics examined. It is an extremely "well behaved" alloy system and presents no experimental handling problems. Sticks of the eutectic composition were prepared from 99.999% purity material by direct melting of the elements under argon. The resulting melt was cast into a permanent, steel mold.

Figure 19 shows transverse and longitudinal sections of this lamellar eutectic. Growth was performed under a temperature gradient of only 5°C/cm at a rate of 20 cm/hr.

B. WHISKER COMPOSITE EXPERIMENTS

The principal objective of the laboratory work on whisker composites was to examine the chemical compatibility of whiskers with Al-based matrices.

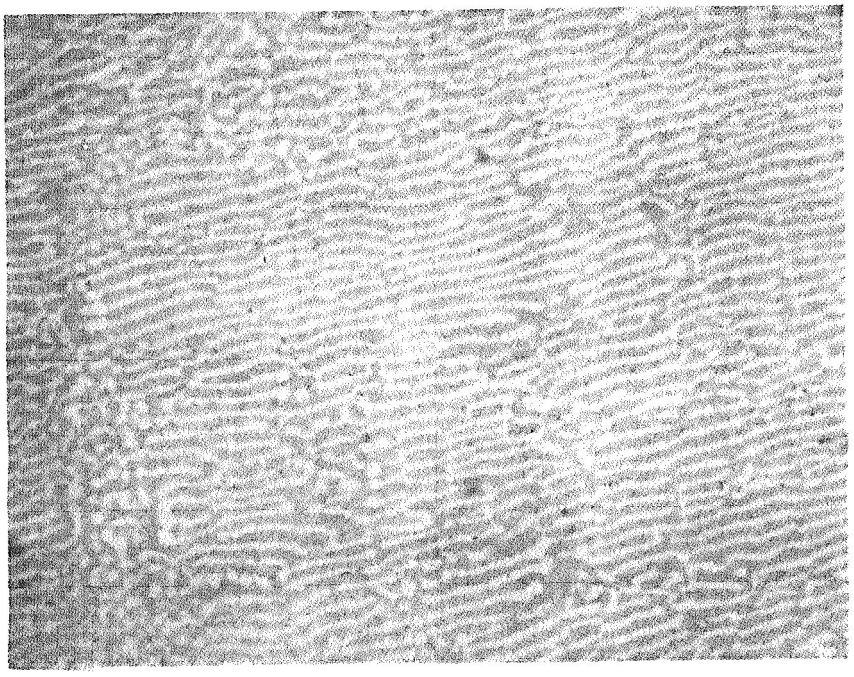

MAG: X 250

FIGURE 17 TRANSVERSE SECTION OF InSb-Sb EUTECTIC (NOTE TENDENCY TOWARD DEGENERATION)

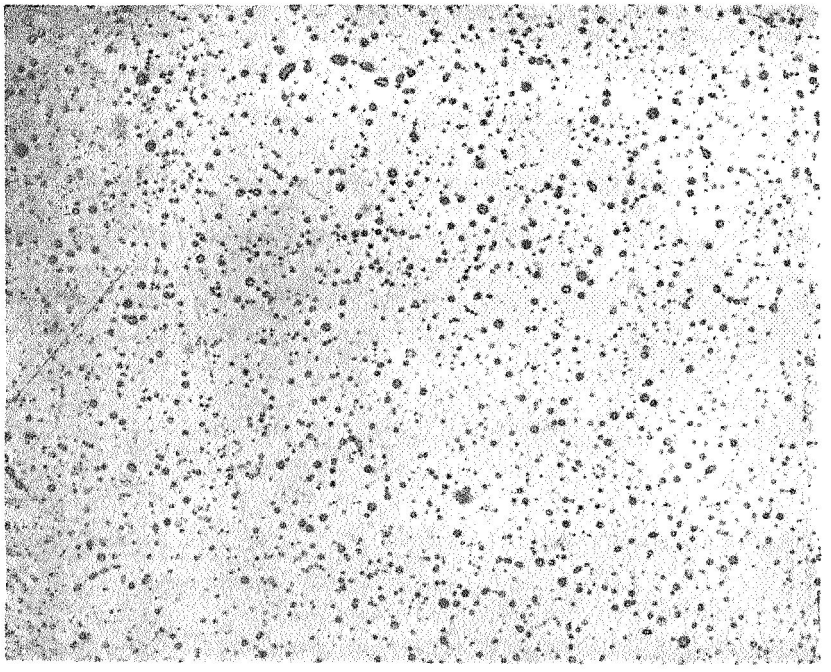

(a) TRANSVERSE SECTION MAG: X 125

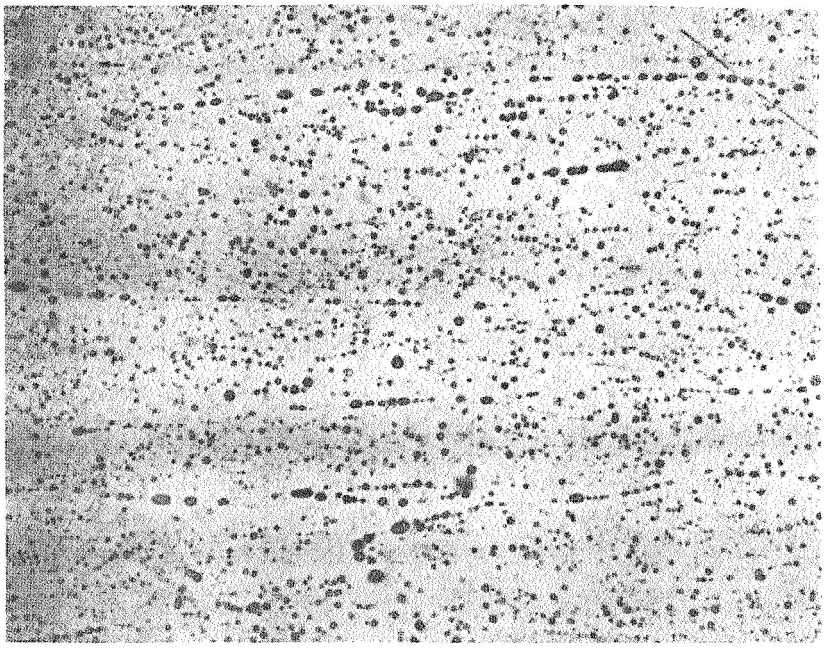

(b) LONGITUDINAL SECTION MAG: X 125

FIGURE 18 PHOTOMICROGRAPHS OF Al-In MONOTECTIC

(a) TRANSVERSE SECTION MAG: X 625

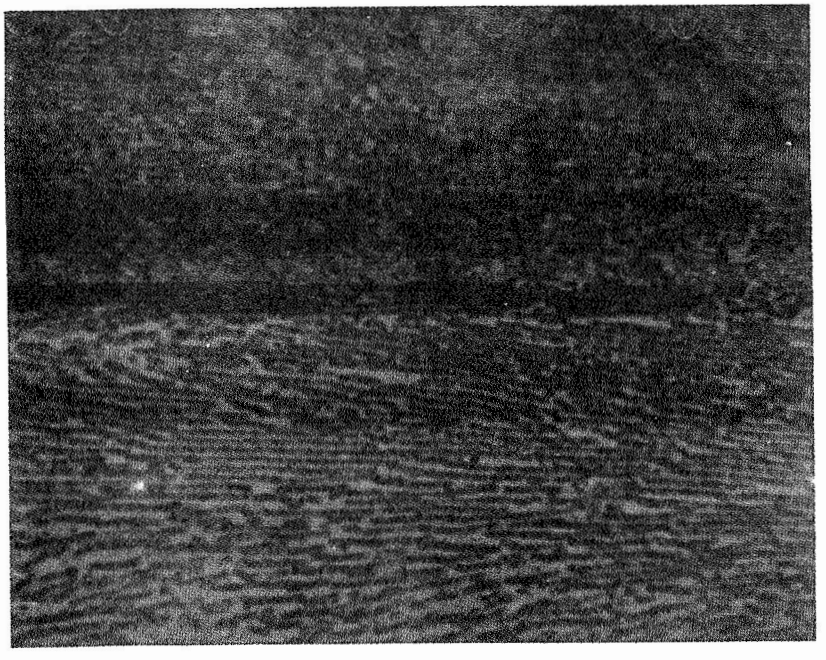

(b) LONGITUDINAL SECTION MAG: X 625

FIGURE 19 PHOTOMICROGRAPHS OF Pb-Sn EUTECTIC

1. SiC Whiskers

Ni-plated α-SiC whiskers were placed in contact with 99.999% pure aluminum (under an argon atmosphere), maintained at the melting point for times of 15 seconds, 30 seconds, 60 seconds and 120 seconds. The whiskers, together with adhering Al, were withdrawn from the crucible and prepared for metallographic examination.

We observed that reaction between the Al and the α-SiC occurred within 1 minute of exposure to the melt. Figure 20 is a photomicrograph of the 2-minute exposure sample; the whiskers have been completely degraded. The reaction product is probably Al_3C_4. These observations suggest that α-SiC whiskers should not be used in the first orbital experiments.

2. Al_2O_3 Whiskers

An Al-Cu eutectic alloy was used as the matrix material for experiments with Al_2O_3 whiskers. The alloy was heated to the melting point in an Al_2O_3 crucible under a flowing argon atmosphere. A small quantity of the coated whiskers was introduced into the melt and the whole assembly stirred using an Al_2O_3 rod. After about 5 minutes, the power was switched off and the melt allowed to solidify in the crucible. One experiment was performed with Mo-coated whiskers and one with Cr-coated whiskers.

We found that wetting occurred more readily with the Mo-coated sample. This may be due, in part, to the more stable oxide film present on the Cr-coated material. Figure 21 is a high-magnification photograph showing a Mo-coated α-Al_2O_3 whisker within a lamellar of Al_2Cu. (The plane of the sector is approximately parallel to that of the interphase boundary of the Al-Al_2Cu eutectic.)

C. DISPERSED COMPOSITE EXPERIMENTS

For simplicity, we used rf heating to melt samples of TD-Ni and TD-Ni-Cr in a manner similar to the sphere forming experiments.

Very poorly developed spheres were obtained from the drop casting experiments. The captive sting experiments were far more successful and relatively smooth surfaces were obtained.

The selection of these materials was based upon the fact that in zero-g, particle agglomeration and separation due to differences in density would be eliminated during melting of the matrix. However, as is shown in Figures 22 and 23 gross agglomeration occurs as a result of the "sweeping" of the thorium oxide particles ahead of the advancing solid fronts during freezing. Particles are swept into the interdendritic regions. While gravity is

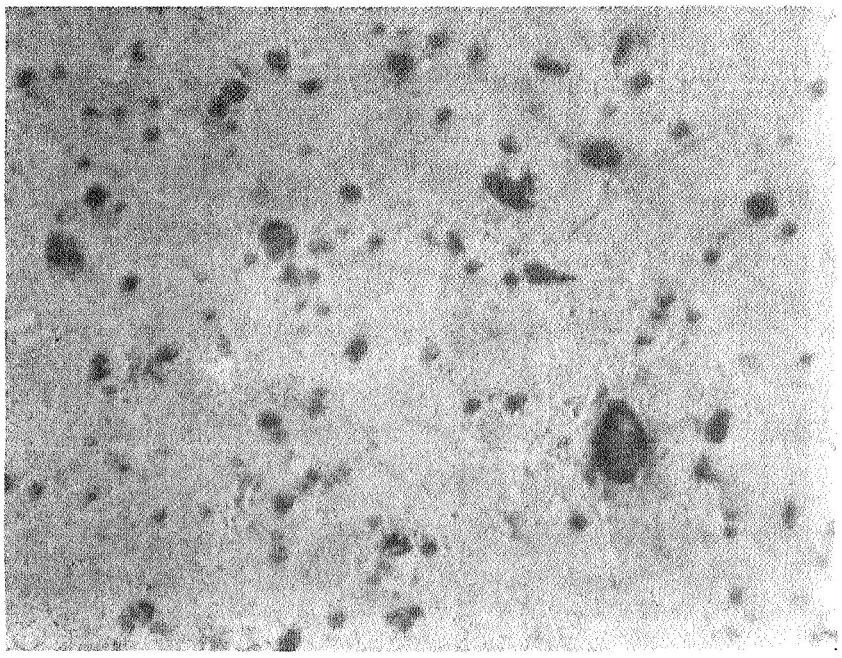

MAG: X 650

FIGURE 20 RESULT OF 120-SEC EXPOSURE OF α-Si C WHISKERS TO MOLTEN Al

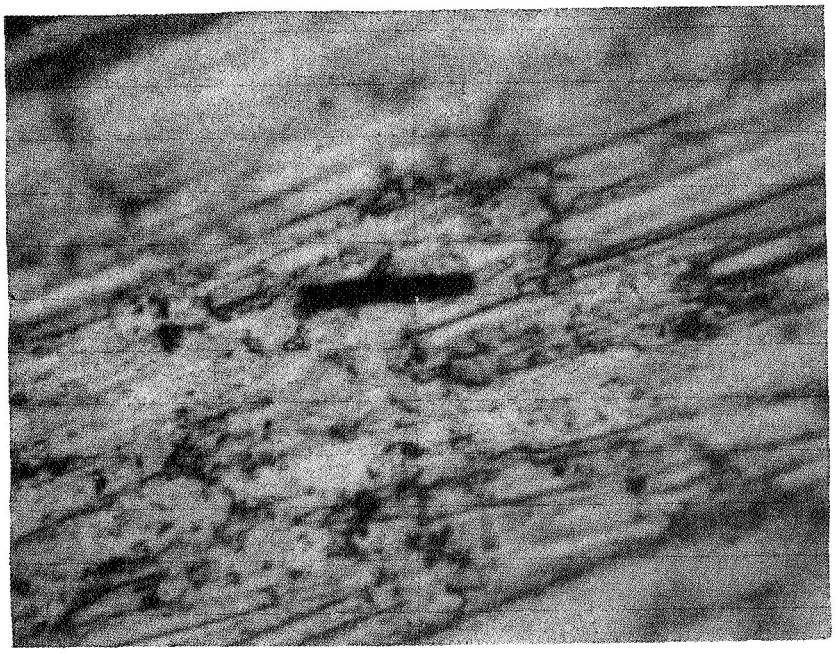

MAG: X 1250 (UNETCHED)

FIGURE 21 PHOTOMICROGRAPH SHOWING SECTION OF Mo-COATED α - Al_2O_3 WHISKER IN A LAMELLAR OF Al_2Cu. (Section approximately parallel to interphase boundary)

MAG: X 62

FIGURE 22 PHOTOMICROGRAPH SHOWING SEGREGATION OF THORIA PARTICLES TO INTERDENDRITIC REGIONS OF A CAPTIVE STING MELT OF THORIA-DISPERSED Ni-Cr

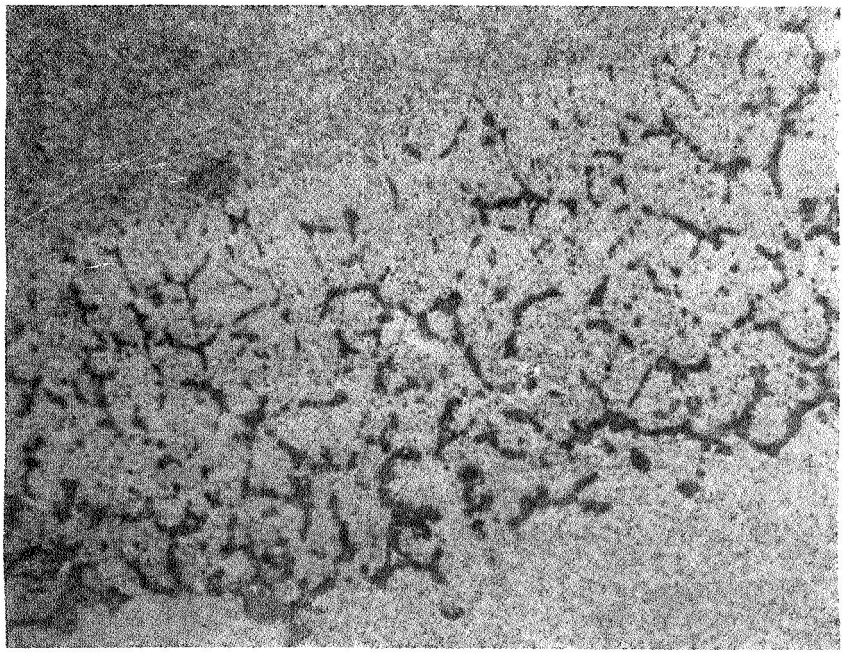

MAG X 625

FIGURE 23 SECTION THROUGH CAPTIVE STING-MELTED THORIA-DISPERSED NICKEL SHOWING GROSS SEGREGATION OF PARTICLES

certainly playing a role in the macroscopic distribution of ThO_2 in the samples represented by Figures 21 and 22, there is little doubt that the "sweeping" effect is predominant and would also exist in zero-g.

D. RECOMMENDATIONS

We believe that a sample of a eutectic and of a monotectic alloy should be included in the first orbital experiment. Al-In seems to be a good choice for the monotectic. It is a simple, low-melting, low-reactivity system and could provide an excellent demonstration of the benefits of the zero-g environment.

Eutectics Al-Cu and Pb-Sn have been extensively studied on earth. Both are lamellar and are very similar in terms of potential success in the orbital experiment. However, Al-Cu is a more useful engineering system than Pb-Sn. Furthermore, the melting temperatures are quite close to that of the Al-In monotectic. This promotes a practical advantage because both Al-In and Al-Cu could be prepared in an exothermal package of the same design. Pb-Sn would require an entirely different thermal profile.

Consequently, we recommend that Al-17.3wt% In monotectic and Al-33wt% Cu eutectic be used in the "directionally frozen composite" experiments.

We recommend that SiC whiskers should not be used because of preparation and compatibility problems. As noted above, α-Al_2O_3 whiskers with a thin surface coating of Mo were readily wetted by the Al-Cu matrix alloy and this system appears to be the best choice for the whisker experiment. There is again a practical advantage in that the matrix for α-Al_2O_3 is the Al-Al_2Cu eutectic, thus facilitating use of the same design of exotherm to that used for the monotectic and eutectic directional freezing experiments.

XIII. PRELIMINARY HARDWARE DESIGN

A. DESIGN CRITERIA

The design of the composite casting experiment is simplified because there are no moving components or sample-positioning requirements. In some respects heat transfer considerations are less critical to the design, and will be provided for in the design of the exothermal heaters. Therefore, the apparatus and samples can be more rugged. The samples will not be freely floating as in the sphere forming experiment.

The experiment will consist of an experiment package which can be stored in an appropriate location outside the experimental chamber until ready for use. The package will contain heating units, each of which constitutes a composite casting experiment. The units will be supported by a framework which is integral with the experiment package. The package will contain and support the units during launch, orbit, and return to earth, and also provide a simple and convenient means for handling the experiment.

The astronaut will remove the experiment package from its storage location, separate its cover, and then mount the experiment on the supports in the vacuum chamber. Our laboratory program and analysis, and information provided by the manufacturer of the exothermal heaters (Whittaker Corp.), resulted in our establishing the following design criteria and principles:

The experiment package must contain the necessary electrical connectors and wiring to permit positive ignition of individual exothermal heaters by the astronaut after the package is positioned within the metal melting facility and the chamber evacuated.

The experiment package must contain suitable provisions for attachment and positioning both within and outside the experimental chamber.

The experiment package must have sufficient venting area so that gaseous products evolved during exotherm burn can be effectively released to the chamber vacuum, either by (a) the package being opened by the astronaut before it is placed inside the chamber, and closed again after the experiment is completed but prior to storage (partial opening could be used or an entire side of the package could be removed) or (b) the package containing vent ports (integral with its construction) of sufficient open area to permit rapid outgassing.

Each experiment unit should contain the exotherm, ignition source, wiring, container, inner liner or sample holder, sample, radiator

assembly, and a means for maintaining it in contact with the sample, a mechanical connection to the experiment package, and inter-unit supports as required.

Each experiment unit, or the experiment package, should provide a means to secure the radiator assembly in the unit during launch, maneuver, and reentry. This will also keep the sample in place.

Each experiment unit preferably should be identical, except for the sample materials, to simplify construction, assembly, operational uniformity, etc. The present selection of sample materials permits use of the same exothermal composition and heating profile.

The experiment units should be arrayed within the package so that uniform temperature profiles will be generated in each experiment.

The experiment units and package should be designed so that the radiator assemblies which provide the temperature gradient in the directional solidification experiments have a uniform view of the cold walls of the chamber. Furthermore, the radiator design and location of the sample package in the chamber must not result in localized overheating of the chamber.

The orientation of the package and the experiment units is not overly critical; however, if there will be residual accelerations in known directions in the chamber, the samples should be mounted so that convective heat transfer would be minimized (i.e., the temperature gradient increasing along the direction of induced acceleration).

B. HARDWARE COMPONENTS

We prepared engineering drawings of the hardware selected for the composite casting experiment. (An artist's conception of the experiment package is shown in Figure 2.) The experiment package is approximately 8 x 9.5 x 6.5 inches and consists of three principal components: a removable cover, a baseplate and support structure, and six exothermal heaters.

The experiment package cover, fabricated from fiberglass, aluminum or other lightweight material, completely encloses the exothermal heaters and is held in place by two quick-release fasteners. Lightening holes and openings for gas release are provided. The astronaut removes the cover prior to placing the experiment package in the Materials Melting Facility.

The baseplate and support structure consists of an aluminum baseplate, four support bolts, and a partition which hold the six exothermal heater assemblies in place. The baseplate and partition may be fabricated of aluminum or stainless steel and be lightened or strengthened as required. An electrical connector is attached

to the baseplate. Wiring from the connector to the exothermal heater ignitors is attached to the baseplate.

The design and fabrication of the exothermal heater assembly is being accomplished by the Whittaker Corp. under separate contract. To assist Whittaker, we conducted measurements to establish the required cooling rates for the directional solidification experiments. The basic components of the exothermal heating assembly are shown schematically in Figure 24. The sample to be melted is contained in a boron nitride crucible held in a stainless steel liner. The exotherm is shaped to provide the required temperature gradient; the finned tungsten rod at the end of the sample also determines the temperature gradient and provides a heat sink. Insulation, another container, and a baseplate with attachment points are provided. A tension spring provides the force to maintain the tungsten heat sink in good contact with the molten sample and to permit thermal expansion. A separate hold-down spring and clamp mechanism attached to the cover holds the sample and tungsten radiator in place during launch, transit, and reentry. The astronaut releases this clamp before the experiment is initiated. The sample is approximately 4 inches long and 1/4 inch in diameter. After the sample is melted, the temperature distribution should be linear from 650°C at the cool end to 950°C at the warm end (30°C/cm gradient). During cooling this gradient should be maintained. The cooling rate should not exceed 8°C/minute. This temperature distribution is adequate for all of the samples to be melted, namely Al-In and Al_2Cu-Al with and without sapphire whiskers. Duplicate samples of each material will be used.

To perform the experiment, the astronaut removes the experiment package from the stowed location, separates the cover from the baseplate, and installs the equipment in the vacuum chamber. After making the electrical connections, he closes the chamber and evacuates it. Exothermal heaters can be ignited in the desired sequence, leaving sufficient time between portions of the experiment for the components to cool. The chamber can be repressurized to accelerate cooling. After all exothermal heaters have been activated, and the equipment cooled, the astronaut removes the baseplate and heaters, reassembles the cover, and stows the package.

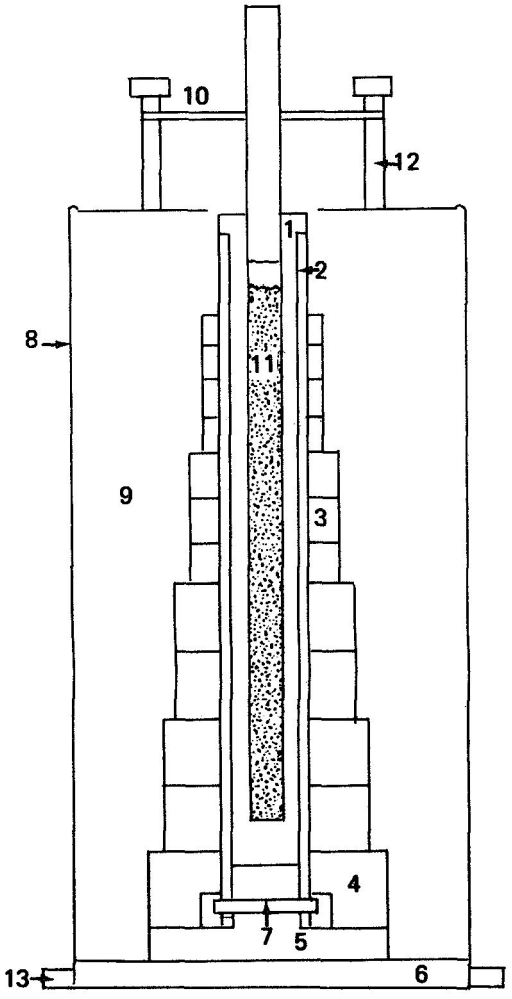

1. BN Crucible
2. SS Crucible Liner
3. Exotherm Rings
4. BN Spacer
5. BN Pedestal
6. Aluminum Base Plate
7. Locking Pin
8. SS Housing
9. Fiberfrax Insulation
10. Tungsten-Finned Heat Sink
11. Sample
12. Spring
13. Attachment Points

FIGURE 24 SCHEMATIC DIAGRAM OF EXOTHERMAL HEATER FOR FLIGHT HARDWARE

XIV. REFERENCES FOR PART THREE

1. H. Hahn, Melpar, Private Communication.

2. A. Kelly and W. R. Tyson: High Strength Materials. ed. by V. F. Zackay, John Wiley, New York (1965).

3. D. L. McDanels. TRANS. AIME 233, 636 (1965).

4. D. W. Petrasek. TRANS. AIME 236, 887 (1966).

5. J. M. Whitney and M. B. Riley. AFML-TR-65-39, AD 619 495, May (1965).

6. R. L. Mehan, Contract AF 33(615)-1696, Annual Summary Report, AD 468 533, Aug. (1965).

7. A. Gotti. Contract AF 33(615)-1644. AFML-TR-65-354, Nov. (1965).

8. S. Rodney and R. Long: Summary Report, U. S. Army Contract DA-04-495-AMC-431(A), Jan. (1965).

9. R. A. Rosenberg, Mitron Co., 899 Main St., Waltham, Mass., Personal Communication.

10. H. W. Rauch, Sr., W. H. Sutton, and L. R. McCreight: Ceramic Fibers and Fibrous Composite Materials. Academic Press, 1968, Contract Report No. 56.

11. A. L. Hoffmanner: Contract NOw 65-0281-f, Final Report, August 12, 1966.

12. I. Ahmad: Contract Report No. 94 in Reference 32.

13. J. D. Livingston and H. E. Cline: TRANS. AIME 245, 351 (1969).

14. G. A. Chadwick: BRIT. J. APPL. PHYS. 16, 1095 (1965).

15. F. S. Galasso: J. OF METALS 19, 17 (1967).

16. W. K. Liebmann and E. A. Miller: J. APPL. PHYS. 34, 2653 (1963).

17. H. Weiss and M. Wilhelm: ZEITSCHRIFT FUR PHYSIK 176, 399 (1963).

18. B. Paul, H. Weiss and M. Wilhelm: Solid-State Electronics, Pergamon Press, Vol. 7, p 835-841 (1964).

19. S. A. Levy, Y. B. Kim, and R. W. Kraft: J. APPL. PHYS. 37, 3659 (1966).

20. J. G. Loxham and A. Hellawell: J. AM. CERAM. SOC. 47, 184 (1964).

21. D. L. Albright: Ph.D. Dissertation, Lehigh University.